A conserved nuclear receptor, Tailless, is required for efficient proliferation and prolonged maintenance of mushroom body progenitors in the *Drosophila* brain

Mitsuhiko Kurusu[1 #], Yasushi Maruyama[2], Yoshitsugu Adachi[2, ¶], Masataka Okabe[3], Emiko Suzuki[1] and Katsuo Furukubo-Tokunaga[2 #]

[1]Structural Biology Center, National Institute of Genetics, and Department of Genetics, The Graduate University for Advanced Studies, 1111 Yata, Mishima, Shizuoka 411-8540, Japan

[2]Graduate School of Life and Environmental Sciences, University of Tsukuba, 1-1-1 Tennodai, Tsukuba 305-8572, Japan

[3]Department of Anatomy, The Jikei University School of Medicine, Minato-ku, Tokyo 105-8461, Japan

¶ Present address:

Department of Cell Biology, Biozentrum, University of Basel, Klingelbergstrasse 70, CH-4056 Basel, Switzerland

 # Corresponding authors:

Mitsuhiko Kurusu; mkurusu@lab.nig.ac.jp, Phone +81-55-981-6813, Fax +81-55-981-6842

Katsuo Furukubo-Tokunaga; tokunaga@sakura.cc.tsukuba.ac.jp, Phone/Fax +81-29-853-6644

Abstract

The intrinsic neurons of mushroom bodies (MBs), centers of olfactory learning in the *Drosophila* brain, are generated by a specific set of neuroblasts (Nbs) that are born in the embryonic stage and exhibit uninterrupted proliferation till the end of the pupal stage. Whereas MB provides a unique model to study proliferation of neural progenitors, the underlying mechanism that controls persistent activity of MB-Nbs is poorly understood. Here we show that Tailless (TLL), a conserved orphan nuclear receptor, is required for optimum proliferation activity and prolonged maintenance of MB-Nbs and ganglion mother cells (GMCs). Mutations of *tll* progressively impair cell cycle in MB-Nbs and cause premature loss of MB-Nbs in the early pupal stage. TLL is also expressed in MB-GMCs to prevent apoptosis and promote cell cycling. In addition, we show that ectopic expression of *tll* leads to brain tumors, in which Prospero, a key regulator of progenitor proliferation and differentiation, is suppressed whereas localization of molecular components involved in asymmetric Nb division is unaffected. These results as a whole uncover a distinct regulatory mechanism of self-renewal and differentiation of the MB progenitors that is different from the mechanisms found in other progenitors.

Keywords: *Drosophila*, mushroom body, neuroblast, ganglion mother cell, stem cell, *prospero*, brain tumor, asymmetric division, proliferation

Introduction

In the course of brain development, a large number of cells are generated by the division of neural progenitor cells, that can self renew and generate both neurons and glia. Proliferation of neural progenitors is thought to be under precise temporal and spatial control by multiple intrinsic and extrinsic factors (reviewed in Gage, 2000; Alvarez-Buylla et al., 2001; Ming and Song, 2005; Hevner, 2006). As a consequence, different sets of progenitor cells have distinctive temporal windows for mitosis during development. Thus, whereas most neurons in the mammalian cortex are generated during embryonic development, the subventricular zone arises as the site of late progenitor division, and prolonged postnatal neurogenesis persists in the subgranular layer of the hippocampal dentate gyrus and the subventricular zone of the lateral ventricle (Gage, 2000; Alvarez-Buylla et al., 2001; Ming and Song, 2005; Hevner, 2006; Noctor et al., 2007). However, exact molecular mechanisms underlying persistent cell proliferation in these restricted cortical zones remain elusive.

The *Drosophila* brain provides an attractive model system to study the molecular and genetic mechanisms of neural progenitor proliferation. During neurogenesis, the neural progenitors, termed neuroblasts (Nbs), undergo asymmetric cell division in a stem cell-like mode to generate a series of smaller daughter cells called ganglion mother cells (GMCs), each of which divides only once to produce a pair of post mitotic neurons or glia cells. Studies of *Drosophila* Nbs have provided insights into the genetic and molecular mechanisms controlling asymmetric cell division (Betschinger and Knoblich, 2004; Yu et al., 2006; Chia et al., 2008; Doe et al., 2008). During the division of Nbs, a conserved protein complex consisting of Par-3/Bazooka, Par-6, and atypical Protein Kinase C (aPKC) establishes the axis of cell polarity and recruits Inscuteable to the apical pole. Thus, apical proteins such as atypical aPKC are selectively partitioned into Nb to promote Nb self-renewal (Rolls et al.,

2003; Lee et al., 2006a), while basal proteins such as Miranda (MIRA), Brain Tumor (BRAT), and Prospero (PROS) are partitioned into GMC to control cellular differentiation (Betschinger et al., 2006; Lee et al., 2006b; Bello et al., 2006).

Like the vertebrate neural progenitor cells, *Drosophila* Nbs generate diverse types of neurons and glia by spatially and temporally controlled mechanisms (Truman and Bate, 1988; Isshiki et al., 2001; Pearson and Doe, 2003; Pereanu and Hartenstein, 2006; Younossi-Hartenstein et al., 2006). During embryonic neurogenesis, Nbs undergo progressive restriction of their competence, which is defined by sequential expression of transcription factors. GMCs and post mitotic neurons maintain the transcription factor profile of the Nbs present at their birth, thereby generating distinctive neural layers in the embryonic nervous system. Moreover, temporal series of transcription factor code extends into postembryonic neurogenesis (Zhu et al., 2006; Maurange et al., 2008). In particular, multiple different neuronal identities are sequentially generated in the mushroom body (MB) and antennal lobe (Lee and Luo, 1999; Jefferis et al., 2001) under gradients of a BTB-Zinc finger protein, Chinmo (Zhu et al., 2006). Intriguingly, temporal transcription factors and their targets also schedule the end of neural proliferation in the postembryonic brain either recruiting PROS into Nb nucleus or inducing Nb apoptosis (Maurange et al., 2008).

The intrinsic neurons of MBs, which constitute most of the MB structure, are generated by four Nbs localized in the posterior dorsal cortex, each of which gives rise to an indistinguishable set of neurons (Ito and Hotta, 1992; Ito et al., 1997). Although most Nbs in the *Drosophila* brain cease postembryonic neurogenesis by early pupal stage, MB-Nbs maintain exceptional proliferation activity that persists until the end of the pupa stage (Fig. 1A and Sup. Fig. 1) (Truman and Bate, 1988; Ito and Hotta, 1992), providing a unique opportunity to study the regulatory mechanism of persistent proliferation of neural

progenitors during brain development.

In this study, we show that *tailless* (*tll*), a member of the orphan nuclear receptor superfamily, is required for efficient proliferation and prolonged maintenance of MB progenitors. Mutations of *tll* progressively impaired cell cycle activity in MB-Nbs and cause premature loss of Nbs in the early pupal stage. TLL is also expressed in MB-GMCs to prevent apoptosis and promote cell cycling. Furthermore, ectopic expression of TLL downregulated PROS in non-MB progenitors, generating brain tumors with supernumerary Nbs. We also show that the activities of *tll* and *pros* are differently required for the control of MB- and non-MB progenitors. These results suggest a unique regulatory mechanism of self-renewal and differentiation in MB progenitor cells that is distinct from the mechanisms regulating neural progenitors of other lineages.

MATERIALS AND METHODS

Fly stocks

The following fly strains were used: wild-type (Oregon-R), OK107 (a Gal4 enhancer trap line for *eyeless* (*ey*) and expressed in the majority of the MB neurons; Connolly et al., 1996, Adachi et al., 2003), *embryonic lethal abnormal vision* (*elav*)-*Gal4* (a pan-neural Gal4 line, Luo et al., 1994), *elav-GeneSwitch-Gal4* (an inducible *elav-Gal4* line, Osterwalder et al., 2001), $ey^{J5.71}$ (Kurusu et al., 2000), $dachshund^{4}$ (*dac*, Mardon et al., 1994), *UAS-mCD8::GFP* (Lee and Luo, 1999), *UAS-GFP* (provided by E. Hafen), tll^{l49} (strong allele; Pignoni et al., 1990), tll^{1} (hypomorphic; Pignoni et al., 1990), *UAS-pros* (provided by F. Matsuzaki), and FRT82B $pros^{17}$ (Reddy and Rodrigues, 1999). *UAS-tll* flies were constructed with the standard pUAST

.

Clonal analyses

Clonal analyses were performed based on the Mosaic Analysis with a Repressible Cell Marker (MARCM) system (Lee and Luo, 1999). The following genotypes were examined. For *tll* mutant clones: *hs-FLP UAS-mCD8::GFP*; FRT82B tll^{l49}/FRT82B *tub-Gal80*; OK107/+ and $Gal4^{c155}$ *hs-FLP UAS-mCD8::GFP*; FRT82B tll^{1}/FRT82B t*ub-Gal80*. For rescue experiments: $Gal4^{c155}$ *hs-FLP UAS-mCD8::GFP*; UAS-*tll*/+; FRT82B tll^{1}/FRT82B *tub-Gal80*. For TLL overexpression experiments: FRT19A/t*ub-Gal80 hs-FLP* FRT19A; *elav-Gal4 UAS-mCD8::GFP*/+; *UAS-tll*/+. For *pros* mutant clones: *hs-FLP UAS-mCD8::GFP*; FRT82B $pros^{17}$/FRT82B *tub-Gal80*; OK107/+. For *pros tll* double mutant clones: *hs-FLP UAS-mCD8::GFP*; FRT82B $pros^{17}$ tll^{l49}/FRT82B *tub-Gal80*; OK107/+. Egg collection was performed for 2-3 h on standard food at 25°C. A single 60 min heat shock at 37°C was

applied in the early first instar stage for the induction of MB clones and in the late first instar stage for the induction of other clones.

Immunohistochemistry and confocal microscopy

Immunostaining of brains were performed as previously described (Kurusu et al., 2000). The following antibodies were used: goat FITC-conjugated anti-horseradish peroxidase (HRP) (1:300; Jackson ImmunoResearch, West Grove, PA, USA), rabbit anti-TLL (1:200; Kosman et al., 1998), rabbit anti-EY (1:300; gift from Dr. Walldorf), mouse anti-DAC (1:20; dac2-3; DSHB) (Mardon et al., 1994), mouse anti-FAS II (1:5; 1D4; DSHB), rabbit anti-phosphohistone H3 (PH3) (1:500; Millipore Corporation, Billerica, MA, USA), mouse anti-Cyc B (1:5; F2F4; DSHB), mouse anti-Cyc E (1:5; 8B10; Richardson et al., 1995), rat anti-Cyc E (1:200; Richardson et al., 1995), mouse anti-PROS (1:50; MR1A; DSHB), rat anti-PROS (1:50; gift from Dr. Matsuzaki), rabbit anti-MIRA (1:2000; Ikeshima-Kataoka et al., 1997), rabbit anti-BRAT (1:200; Betschinger et al., 2006), rabbit anti-PINS (1:1000; Izumi et al., 2006), rabbit anti-aPKC (1:400; Santa Cruz Biotechnology, Santa Cruz, CA, USA), rat anti-mCD8α (1:100; Invitrogen, Carlsbad, CA, USA), and FITC-, Cy3- or Cy5-conjugated secondary antibodies (1:400; Jackson ImmunoResearch, West Grove, PA, USA). Confocal images were captured with a Zeiss LSM410 or LSM510 confocal microscope. Optical sections were obtained at 1-2 μm intervals. Images were processed digitally and then arranged with Adobe Photoshop.

TUNEL assay

Apoptotic cells were detected with Apotag kit (Millipore Corporation, Billerica, MA, USA). Freshly dissected brains were fixed for 30 min in 4% paraformaldehyde in PBS, washed three

times in 0.1% PT, and then equilibrated for 30 min in the equilibration buffer supplied with the kit. Brains were then incubated with terminal transferase mixture for 1 h at 37°C, washed three times for 10 min at 37°C in the stop buffer, and incubated for overnight at 4°C with Texas Red-conjugated anti-digoxigenin antibody diluted 1:1 with the blocking solution.

BrdU labeling

For BrdU incorporation into dissected post-embryonic brains, each of the developmentally-staged brains were dissected in PBS and immediately labeled with 37.5 µg/ml BrdU (GE Healthcare, Little Chalfont, Buckinghamshire, UK) in *Drosophila* SFM solution (Invitrogen, Carlsbad, CA, USA) for 1 h. After 30 min fixation with 4% PFA in PBS, brains were treated with 2 N HCl for 1 h at room temperature. BrdU of the embryonic central nervous system (CNS) was performed as previously described (Richardson et al., 1993). Briefly, embryos were dechorionated with bleach, permeabilized with octane for 4 min, and then soaked in BrdU solution (1 mg/ml in PBS) for 30 min at 25°C. After 30 min fixation with 4% PFA in PBS, embryos were devitellinized by hand peeling with forceps, treated with 2 N HCl for 1 h at room temperature. Incorporation of BrdU was monitored with an anti-BrdU (1:250; Becton Dickinson, Franklin Lakes, NJ, USA) staining. For BrdU pulse-chase experiments, newly molted third instar larvae were fed a standard food containing 750 µl/ml BrdU for 3 h; for an immediate examination, these larvae were dissected and processed for BrdU labeling, for a chase examination, another pool of BrdU-treated larvae were grown without BrdU for 32 h before dissection and BrdU labeling.

GeneSwitch

Induction of *elav-GeneSwicth-Gal4* was performed as previously described (Osterwalder et

al., 2001). Briefly, newly molted third instar larvae were fed with RU486 food containing 80 μg/ml RU486 (Sigma-Aldrich, St. Louis, MO, USA), and dissected at the late third instar or 40h after puparium formation (APF). The brains were examined for BrdU incorporation or antibody staining.

Results

TLL expression correlates with the proliferation pattern of the MB progenitors

The MB neurons (Kenyon cells) are generated by four MB-Nbs that divide throughout embryonic, larval, and pupal development (Fig. 1A) (Truman and Bate, 1988; Ito and Hotta, 1992; Tettamanti et al., 1997; Kurusu et al., 2000; Noveen et al., 2000). The MB-Nbs were clearly observed at the embryonic stage 16 at the anterior end of each brain hemisphere (Sup. Fig. 1A). While most of the other neuroblasts ceased dividing between the late embryonic and early first instar stages, the MB-Nbs continued to proliferate (Sup. Fig. 1B). The MB-Nbs continued to divide through the larval stage, in which increasing numbers of other Nbs became active (Sup. Fig. 1C and D). The number of active Nbs rapidly declined between 20 and 30 h APF (Sup. Fig. 1E). By 40 h APF, only four MB-Nbs were left active in the entire brain (Sup. Fig. 1F). The MB-Nbs remained active until the end of the pupal stage (Sup. Fig. 1G), but disappeared in the newly eclosed adult (Sup. Fig. 1H).

To understand the molecular mechanisms underlying the persistent proliferation of MB-Nbs, identification of genes that exhibit correlative expression in the dividing MB-Nbs would provide important clues. As a candidate of such genes, we found that *tll* was expressed in the dividing MB-Nbs and GMCs, but not in the postmitotic neurons, through the stages of MB development. TLL expression is initially found in almost all procephalic neuroblasts (Younossi-Hartenstein et al., 1997; Urbach and Technau, 2003), but became largely restricted to anterior cells by stage 16 (Fig. 1B and B1). Double immunostaining with an anti-DAC antibody, which labels MB neurons (Fig. 2A1; Kurusu et al., 2000; Martini et al., 2000; Noveen et al., 2000), confirmed that they were MB-Nbs and GMCs. In the larval stages, TLL was expressed in the MB-Nbs and GMCs (Fig. 1C-E) as well as in lamina precursor cells (open arrowhead in Fig. 2D). While the expression in lamina precursor cells

disappeared by the end of the larval stage, TLL expression in the MB progenitors was maintained during the pupal stages (Fig. 2F-H). In newly eclosed flies, TLL expression was found in a few GMC-like cells in the middle of the MB cell clusters (Fig. 2I), although their exact identity is unknown.

Mutations of *tll* lead to reduced MB clones

Since the expression profile of TLL correlated well with the mitotic activity of MB-Nbs and GMCs, we determined whether TLL was required for proliferation of the MB progenitor cells using the MARCM system that allows positive labeling of mutant cells (Lee and Luo, 1999). While wild-type clones consisted of more than 200 neurons at the late third instar stage (Fig. 2A), *tll* mutant clones exhibited a dramatic reduction in the numbers of neurons (Fig. 2B and C): 17.2 ± 0.9 cells for tll^{1} (n=40), a hypomorphic allele, and 8.7 ± 0.4 for tll^{l49} (n=117), a strong null allele.

The total number of MB neurons is estimated about 2500 per hemisphere in the adult brain (Technau and Heisenberg, 1982; Ito and Hotta, 1992). Each of the four MB-Nbs accompanies over 500 neurons, which project into three sets of lobes: γ, α'/β', and α/β (Fig. 2D). By contrast, the number of neurons barely increased from the third instar stage in the *tll* mutant clones (10.4 ± 1.1, n=14 for tll^{l49}). In addition, axonal projections of the tll^{l49} clones in the adult brain were restricted to the lobes of larval origin; mostly to the γ and faintly to the α'/β' lobes (Fig. 2E), supporting the notion that neural production had been arrested by the end of the larval stage. On the other hand, the remaining mutant neurons formed wild type-like lobes and calyces in both the larval (Fig. 2B and C) and the adult stages (Fig. 2E), suggesting that *tll* is not required for neuronal differentiation Moreover, EY and DAC, key regulators for neuronal differentiation of the MB neurons (Kurusu et al., 2000;

Martini et al., 2000; Noveen et al., 2000; Callaerts et al., 2001), were expressed in the mutant MB clones as in the wild-type clones (Sup. Fig. 2A-E). Conversely, neither *ey* nor *dac* mutations altered TLL expression (Sup. Fig. 2E-G), suggesting that *tll* is transcriptionally independent of *ey* and *dac*. Finally, the MB defects were rescued by *tll* transgene expression (Fig. 2F, 108 ± 14.2 cells per clone, n=7), confirming that the observed MB defects were indeed caused by lack of *tll* activity.

TLL is required for optimum cell division activity and prolonged maintenance of MB-Nbs

To gain insights into the mechanisms by which *tll* controls cell proliferation, we examined the cellular fate and patterns of DNA synthesis of wild-type and mutant MB-Nbs. Wild-type MB clones always contained a single large Nb during the larval and pupal stages (Fig. 3A). Likewise, a single MB-Nb was found in tll^{l49} clones at the late third instar stage (63/63 clones) and at 20 h APF (38/38 clones) (Fig. 3B). However, none of the mutant MB clone accompanied identifiable Nbs at 40 h APF (0/7 clones) (Fig. 3B). The majority of wild-type MB-Nbs incorporated BrdU during the larval and pupal stages (>80%) (Fig. 3C). In contrast, the fraction of MB-Nbs labeled by BrdU was markedly reduced in tll^{l49} clones at both the larval and the pupal stages (58%, n=24, at the third instar stage and 50%, n=8, at 20 h APF) (Fig. 3C). Moreover, fractions of PH3-positive MB-Nbs were markedly reduced at 20 h APF in tll^{l49} clones (8.7%, n=23), while more than 30% of wild-type MB-Nbs remained PH3 positive through the larval and the pupal stages (Fig. 3C).

To analyze cell cycle defects in *tll* mutant clones, we then examined expression of Cyclin E (Cyc E) and Cyclin B (Cyc B), the principal G1-S and G2-M phase regulators, respectively. Both proteins were constitutively expressed in the wild-type MB-Nbs at the

larval and the pupal stages (Fig. 3D-E, H-I, and L). No difference was found at the third instar stage for *tll*^{l49} mutant MB-Nbs; all MB-Nbs expressed both Cyc E and Cyc B (Fig. 3F-G and L). However, only 50% of the *tll*^{l49} mutant Nbs expressed Cyc B at 20 h APF, whereas all wild-type Nbs expressed the protein (Fig. 3J-K and L). Taken together, these results suggest tha**t** TLL is required for optimum cell cycle progression in MB-Nbs and their prolonged maintenance beyond the early pupal stage.

TLL prevents apoptosis and promotes cell cycle progression in MB-GMCs

Although cell cycle progression of the MB-Nbs is affected in the *tll* mutant clones, the result that a large fraction of the mutant MB-Nbs retained mitotic activity at the late larval stage (Fig. 3) was contradictory to the profound reduction in the larval clone size (see Fig. 2B and C). To further investigate the underlying mechanism, we examined the dividing activity and cellular fate of the mutant MB-GMCs. Intriguingly, compared to wild-type clones, the number of BrdU-labeled GMCs was significantly reduced in the *tll*^{l49} MB clones at the late larval stage (left panel of Fig. 4A) (8.2 ± 0.2, n=31 for WT; 4.0 ± 0.5, n=22 for *tll*^{l49}). Similarly, the number of MB-GMCs labeled with either anti-PH3 or Cyc E was significantly reduced: PH3 (2.4 ± 0.2, n=67 for WT; 1.1 ± 0.1, n=39 for *tll*^{l49}) and Cyc E (3.0 ± 0.2, n=10 for WT; 0.4 ± 0.1, n=14 for *tll*^{l49}). Moreover, *tll* mutant clones accompanied only one BrdU-labeled GMC at 20h APF (right pane of Fig. 4A; 5.4 ± 0.3, n=12 for WT; 1.0 ± 0.4, n=8 for *tll*^{l49}), which was lost by 40 h APF while wild-type clones retained three to four GMCs even at 60h APF (Fig 4A).

To determine the cellular fate of the mutant MB-GMCs, we performed BrdU pulse-chase experiments. A 3 h pulse at the early third instar stage led to BrdU incorporation in 9.0 ± 0.7 MB-GMCs (n=6) in wild-type larvae (Fig. 4B and F). After a 32

h chase, BrdU labeling was found in many postmitotic MB neurons (17.0 ± 0.9, n=7) (Fig. 4C and F). On the other hand, a 3 h pulse labeled only 3.8 ± 0.3 GMCs (n=12) in *tll* mutant MB clones (Fig. 4D and F). Moreover, most of the labeled cells were lost after 32 h chase (0.4 ± 0.3, n=11) (Fig. 4E and F). To determine whether GMCs were indeed lost by cell death in the mutant MB clones, we performed TUNEL labeling experiments. TUNEL positive cells were rare in the wild-type MB clones (0.12 ± 0.04, n=63 at the third instar stage; 0.13 ± 0.07, n=23 at 20 h APF) (Fig. 4G-H and K). However, significant numbers of cells, all of which were GMCs, were TUNEL positive in the tll^{l49} MB clones (0.95 ± 0.25, n=23 at the third instar stage; 1.67 ± 0.56, n=6 at 20 h APF) (Fig. 4I-J and K). In contrast, no TUNEL labeling was detected for the MB-Nb and the postmitotic MB neurons (Fig. 4I and J). To investigate whether the MB-GMC death was mediated by the conventional cell death program, we tried to rescue the defective GMCs by expressing cell death inhibitors. However, the GMC death caused by *tll* mutation was not rescued by either p35 (Sup. Fig. 3) nor Diap1 (data not shown), whereas expression of these inhibitors did suppress cell death in the developing ommatidia (data not shown).

Overexpression of TLL causes brain hyperplasia

To further gain insights on TLL functions in the control of neural progenitor cells, we performed gain-of-function (GOF) analysis using a conventional *elav-Gal4* driver, which drives *Gal4* in all the neural cells including the Nbs and GMCs, but not glial cells (Kurusu et al., 2002; Dumstrei et al., 2003). Unexpectedly, ectopic expression of TLL with *elav-Gal4* in the mid to late embryonic stages caused marked hyperplasia of both the brain and the ventral nerve cord (Sup. Fig. 4A-D). Aberrant cell proliferation in the embryonic CNS was also confirmed by BrdU and PH3 double labeling experiments (Sup. Fig. 4E-H). The

dominant *tll* function in the stimulation of cell proliferation was not restricted to the embryonic stages; ectopic expression of TLL during the third instar stage by an inducible *elav-GeneSwitch* driver (Osterwalder et al., 2001) also stimulated cell division in the larval brain (Fig. 5A and Sup. Fig. 5A-B). Again, an aberrant number of mitotic cells were confirmed by immunolabeling for BrdU, Cyc E, Cyc B and PH3 (Fig. 5B-G).

To determine the cellular identity of aberrant dividing cells, we performed antibody staining for MIRA and PROS. In wild-type Nbs, MIRA localized to the Nb cortex and segregated into GMC, whereas PROS, which plays a crucial function in progenitor differentiation (Betschinger et al., 2006; Lee et al., 2006b; Bello et al., 2006; Choksi et al., 2006), was detected in the nuclei of the GMCs and neurons (Sup. Fig. 5C). Notably, expression of TLL caused a marked increase of MIRA positive cells in the brain (Fig. 5I and J), seemingly at the expense of PROS expressing cells. Intriguingly, many of the MIRA positive cells were heterogeneous in size and found next to each other, yet they all expressed MIRA in their cortex and lacked nuclear PROS (arrowheads in Sup. Fig. 5D), suggesting that they were supernumerary Nbs.

Because our results suggested that *tll* might be required for efficient proliferation and prolonged maintenance of MB-Nbs (Fig. 3), we then examined whether TLL expression resulted in proliferation of non-MB Nbs in the mid pupal stage (40 h APF). No dividing cells were observed in the wild-type brain except for the four MB-Nbs (Sup. Fig. 5E and F). However, TLL overexpression resulted in a large number of dividing cells in the pupal brain (Fig. 5A and Sup. Fig. 5G and H), indicating an aberrant mitotic activity of non-MB progenitors beyond the early pupal stage, by which all of the non-MB progenitors normally cease cell division.

TLL overexpression generates supernumerary-Nb clones without altering cellular polarity

To further analyze the underlying cellular mechanisms of brain hyperplasia caused by TLL, we examined the effect of TLL overexpression in MARCM clones. Wild-type Nb clones always contained a single MIRA-positive and PROS-negative Nb of large to intermediate sizes, which accompanied several PROS-positive GMCs (Fig. 6B, C, and E). In contrast, TLL overexpressing clones often contained multiple MIRA-positive and PROS-negative cells (Fig. 6B, D, and F). The recovery of multiple-Nb clones varied in different Nb lineages (Fig. 6A and B); the Nb lineages of CM (centromedial: according to Pereanu et al., 2006), BLP (basolateral posterior), and DPM (medial dorsoposterior) regions produced clones containing several large to intermediate-sized Nbs (Fig. 6D, F and Sup. Fig. 6), whereas DPL (lateral dorsoposterior) and MB clones never produced multiple Nbs (Sup. Fig. 7B and D). The MIRA-positive and PROS-negative cells in the multiple Nb clones were heterogeneous in size, recapitulating the composite cellular property of the gross hyperplasia brain (see Fig. 5I and Sup Fig. 5D). Notably, axons derived from each of the multiple Nb clones converged into a unified bundle, an indication of clonal integrity (data not shown).

Because the supernumerary Nb phenotype induced by TLL is reminiscent of brain tumors observed in asymmetric division mutants (Rolls et al., 2003; Lee et al., 2006a; Betschinger et al., 2006; Lee et al., 2006b; Bello et al., 2006; reviewed in Yu et al., 2006), we then examined the localization of aPKC, PINS, and BRAT, which are key components controlling asymmetric Nb segregation and cell type specification. Notably, TLL expressing Nbs exhibited normal cortical localization of aPKC, PINS, and BRAT, as well as MIRA (Sup. Fig. 8). These data thus indicate that TLL generate supernumerary Nbs without affecting the expression and the localization of the molecular components involved in asymmetric Nb

division.

Distinctive requirements of *pros* and *tll* in MB- and non-MB progenitors

Previous studies have demonstrated that transcriptional regulation mediated by *pros* is one of the key processes that control proliferation and differentiation of neural progenitors (Betschinger et al., 2006; Lee et al., 2006b; Bello et al., 2006; Choksi et al., 2006; Doe, 2008). In addition, a burst of nuclear PROS expression determines the end of Nb proliferation scheduled by temporal transcription factors (Maurange et al., 2008). We therefore investigated *pros* requirement in MB progenitors. PROS was co-expressed with TLL in the wild-type MB-GMCs (arrowhead in Fig. 7A) but not detected in the MB-Nbs (arrow in Fig. 7A). Consistent with previous studies (Betschinger et al., 2006; Lee et al., 2006b; Bello et al., 2006; Choksi et al., 2006), loss of function (LOF) of *pros* resulted in tumor-like clones of non-MB lineages generating multiple Nb-like cells (64/67, Sup. Fig. 9C). By contrast, none of the *pros* mutant MB clones were transformed into a tumor accompanying only a single Nb (113/113, Sup. Fig. 9D).

Notably, premature termination of MB-Nbs in *tll* mutants (Fig. 3) dose not seem to be mediated by *pros* upregulation in MB-Nbs because PROS expression was not altered in the *tll* mutant clones (Fig. 7B). Conversely, TLL expression was not altered in *pros* LOF clones of either non-MB (Sup. Fig. 9E) or MB (Sup. Fig. 9F) lineages. We also analyzed *tll* and *pros* double mutant clones. Intriguingly, the double-LOF mutations resulted in a *tll*-LOF-like phenotype for MB clones with reduced numbers of neurons (Fig. 7C; 18.6 ± 2.7 neurons), and a *pros*-LOF-like tumor phenotype for non-MB clones with multiple Nbs (Fig. 7D). These data suggest that the proliferation of the MB progenitors is controlled by a mechanism distinct from the mechanism that controls non-MB progenitors, and that

proliferation of Mb-Nbs might be controlled by a *pros*–independent mechanism. Indeed, PROS was kept repressed in the wild-type MB-Nbs even at the end of the pupal stage, when the MB-Nbs terminate proliferation (Sup. Fig 10). None of the MB-Nbs showed PROS upregulation at either 88h (29/29) or 92 h APF (8/8) before their disappearance. Moreover, *pros* LOF MB clones cease cell division by the end of the pupal stage (data not shown).

We further examined GOF interactions of *pros* and *tll* in non-MB lineages. As expected by the downregulation of PROS in TLL overexpression brains (Fig. 5 and 6), simultaneous expression of PROS with TLL suppressed the TLL-induced brain hyperplasia (Fig. 7E-G). We thus conclude that downregulation of PROS is the major cause of the TLL-induced tumorigenic phenotype.

Discussion

The intrinsic neurons of MBs are generated by a specific set of Nbs that originate from the embryonic stage and exhibit uninterrupted proliferation till the end of the pupal stage. In the present study, we have demonstrated that an orphan nuclear receptor, TLL, is required for efficient proliferation and prolonged maintenance of MB-Nbs during MB development. In addition, TLL is expressed in MB-GMCs to suppress cell death and promote cell cycling. On the other hand, ectopic expression of TLL in non-MB lineages causes brain tumors, in which PROS, a homeodomain-containing transcription factor, is downregulated and supernumerary Nbs are generated. These results as a whole uncover a distinct regulatory mechanism of self-renewal and differentiation of the MB progenitors that is different from the mechanisms found in other progenitors.

TLL is required for optimum cell cycle progression and maintenance of MB progenitors

Several lines of evidence indicate that TLL is cell autonomously required for efficient proliferation activity MB-Nbs. BrdU labeling experiments demonstrate that DNA synthesis is partially suppressed in *tll* mutant Nbs in both the larval and the pupal stages (Fig. 3A-C). Cell cycle defects in the mutant MB-Nbs are not evident in the larval stage but confirmed by marked suppression of PH3 (Fig. 3C) and Cyc B activity (Fig. 3K and L) at 20h APF before the disappearance of mutant Nbs. As a whole, these data suggest that TLL is required to maintain efficient cell cycle progression in MB-Nbs, particularly in the pupal stage. On the other hand, although the premature loss of the mutant Nbs might be a consequence of cell cycle exit as has been suggested with other Nbs (Maurange et al., 2008), the exact mechanism of the disappearance of mutant MB-Nbs in the early pupal stage is unknown. It is also plausible that mutant Nbs are removed by apoptosis, as is the case with mutant GMCs,

although we failed to detect TUNEL signals for MB-Nbs at 20h APF, shortly before their disappearance whereas cell death signals in GMCs are evident at both the larval and pupal stages (Fig. 4 I and J).

Despite marginal reduction in cell division activity of MB-Nbs at the larval stage, loss of *tll* activity results in significant reduction of the larval MB clones (Fig. 2B and C). Instead, our results demonstrate that cell cycle progression is impaired in larval MB-GMCs (Fig. 4A). Moreover, the majority of the MB-GMCs are lost by cell death (Fig. 4B-K). The molecular mechanism underlying these GMC defects is yet to be investigated, but it is unlikely that they are mediated by altered PROS expression since PROS is co-expressed with TLL in wild-type MB-GMCs (Fig. 7A), and its expression is unaltered in mutant GMCs (Fig. 7B). In addition, the results demonstrating that neither p35 nor Diap1 rescues GMC death (Sup. Fig 3) suggest that TLL might be involved in suppression of an unconventional cell death pathway.

What is the molecular function of TLL in the regulation of MB progenitors? The fact that TLL is a transcription factor localized in the nucleus suggests that TLL might specify neuronal identity of MB progenitors by regulating cell-type specific genes. However, unlike other regulatory factors that confer either spatial or temporal identity, TLL is expressed only in Nbs and GMCs, and mutant neurons exhibit wild-type like dendritic and axonal wiring patterns even in the adult stage (Fig. 2E), in which perdurance of wild-type *tll* activity in the mutant clones is unlikely. Rather, TLL might provide MB progenitors with cellular identity that specify a distinctive proliferation pattern, either by promoting cell cycle or by preventing apoptosis or by both in parallel. In any case, such identity cannot be determined by TLL on its own because TLL is expressed in other neuronal progenitors such as lamina precursor cells in the optic lobes (Fig. 1D). Instead, we presume that the proliferation identity of MB

progenitors may be specified in combination with other regulatory factors such as EY, which is expressed in MB-Nbs, GMCs and postmitotic neurons to control MB development (Kurusu et al., 2000; Noveen et al., 2000; Callaerts et al., 2001).

In the course of MB proliferation, TLL might downregulate key regulatory genes involved in cell-cycle exit and differentiation, particularly given the fact that TLL functions mostly as a repressor in the early embryogenesis (Moran and Jimenez, 2006). One such candidate gene is *pros.* PROS is detected in MB-GMCs, but not MB-Nbs (Fig. 7A). However, loss of *pros* causes neither tumorous transformation of MB progenitors (Sup Fig. 9D) nor suppression of *tll* phenotype in *pros tll* double mutant clones (Fig. 7E). Moreover, PROS is not upregulated in *tll* mutant clones (Fig. 7B). Thus, these data argue against the involvement of *pros* in the regulation of MB progenitors although they do not exclude a redundant mechanism involving PROS cooperating with other factors. Alternatively, TLL could indirectly control cell cycle progression by downregulating genes that suppress progenitor division. In support of this, it is noteworthy that the mammalian homolog *Tlx* (*NR2E1*) represses a tumor suppressor gene, *Pten,* via consensus TLL/TLX binding sites located in the *pten* promoter, and thereby indirectly stimulates the expression of various cell cycle genes including *Cyclin D1, p57 kip2*, and *p27 kip1* (Miyawaki et al., 2004; Zhang et al., 2006).

Distinct proliferation control in MB progenitors

Studies on *Drosophila* neural progenitors reveal heterogeneity among the brain Nbs in terms of temporal windows of cell division, patterns of self-renewal, and susceptibility to mutations that regulate proliferation and termination of progenitors (Bello et al., 2003; Maurange and Gould, 2005; Almeida and Bray 2005; Cenci and Gould, 2005; Bello et al., 2008; Bowman et

al., 2008; Boone and Doe, 2008). Among the Nbs in the *Drosophila* brain, MB-Nbs exhibit a highly unique proliferation pattern. Most Nbs pause cell division between the late embryonic and the early first instar stages, and cease proliferation by the early pupal stage. By contrast, MB-Nbs divide continuously from the embryonic stage till the end of pupal stage (Ito and Hotta, 1992), generating diverse identities of neurons by temporal order (Lee and Luo, 1999; Zhu et al., 2006). In house cricket (Cayre et al., 1994) and moth (Dufour and Gadenne, 2006), proliferation activity of MB-Nbs further extends beyond the pupal stage to exhibit persistent neurogenesis during adult life.

Although our data clearly indicate a pivotal function of TLL for persistent proliferation and maintenance of MB-Nbs, the mechanism that determines the exit from cell cycling at the end of pupal stage remains elusive. Neither extension of TLL expression beyond the end of the pupal period nor blocking cell death program, by p35 or Diap1, prolonged MB-Nb proliferation beyond the pupal stage (our unpublished observation), suggesting existence of other mechanisms that schedule the end of MB-Nb activity. In most brain Nbs, a burst of PROS in the nucleus at around 120 h after larval hatching (24 h APF) induces cell cycle exit to regulate generation of postmitotic progeny in the brain (Maurange et al., 2008). However, no burst of nuclear PROS is detected for MB-Nbs at the end of the pupal stage when they finally exit from cell cycling (Sup Fig. 10), although our data demonstrate that, as is the case with other Nbs in the brain, PROS indeed has such regulatory potential in larval MBs that its overexpression results in partial loss of the MB-Nbs (Sup. Fig. 11). Moreover, MB clones lacking *pros* activity, which exhibit normal growth (Sup. Fig. 9D), cease cell division by the end of the pupal stage (data not shown).

During asymmetric cell division of *Drosophila* Nbs, PROS is kept inactive by tethering to the cell cortex by MIRA (Betschinger and Knoblich, 2004; Bello et al., 2006;

Betschinger et al., 2006; Lee et al., 2006b; Yu et al., 2006; Chia et al., 2008; Doe et al., 2008). At telophase of Nb cell cycle, PROS is segregated into GMC, where it enters the nucleus to trigger cell cycle exit and promote differentiation of post mitotic progeny that are generated by the division of GMC. Accordingly, nuclear PROS is expressed at high levels in postmitotic neurons and at moderate levels in GMCs (Bello et al., 2006). However, whereas this partition pattern of PROS in the post-embryonic brain is shared between MB and non-MB progenies (Fig. 6, Sup. Fig. 7 and Fig. 7A), PROS seems dispensable for cell-cycle control of MB-GMCs (Sup. Fig. 9D). In non-MB lineages, loss of *pros* activity in GMCs leads to failure of cell-cycle exit and transforms of GMCs into Nbs (Sup. Fig. 9C; Bello et al., 2006; Betschinger et al., 2006; Choksi et al., 2006). However, loss of *pros* activity never causes transformation of MB-GMCs (Sup. Fig. 9D) although mutant MB neurons exhibit considerable dendritic defects (data not shown). On the other hand, as we discussed above, TLL is expressed and required for MB-GMCs to suppress apoptosis and maintain active cell cycling. Intriguingly, whereas PROS is suppressed by TLL in non-MB progenitors (Fig. 5 and 6), both proteins are coexpressed in MB-GMCs (Fig. 7A), clearly suggesting that, as compared to the progenitors of non-MB lineages, a different mechanism may operate in MB progenitors to control the expression of regulatory factors that are important for cell division and differentiation.

Brain tumors produced by ectopic expression of TLL

The brain hyperplasia produced by TLL overexpression was reminiscent of brain tumors caused by mislocalization of asymmetric determinants. Aberrant Nb divisions that disrupt the positioning of such factors generate brain tumors (Yu et al., 2006; Chia et al., 2008). Brain tissues from *pins, mira, numb,* or *pros* mutants generate tumors when transplanted in

the wild-type abdomen (Caussinus and Gonzalez, 2005). In double mutants of *pins* and *lgl*, mislocalization of aPKC in the basal cortex results in the generation of supernumerary Nbs at the expense of GMCs, and thus, neurons (Lee et al., 2006a). BRAT is required for the asymmetric positioning of PROS, which in turn suppresses self-renewal of GMC and promotes cell differentiation by transcriptional control (Choksi et al., 2006). Mutant clones of either *brat* or *pros* are highly tumorigenic, forming a large number of MIRA-positive Nbs (Lee et al., 2006b; Bello et al., 2006; Betschinger et al., 2006).

While recapitulating the tumor phenotype, ectopic expression of TLL does not affect asymmetric localization of aPKC, PINS, and BRAT (Sup. Fig. 8). Instead, TLL downregulates PROS in hyperplasic brains (Fig. 5I) and in overexpression clones (Fig. 6D and F), suggesting that the tumorigenesis phenotype caused by TLL expression is mediated by PROS downregulation in GMCs. This notion is further supported by the fact that coexpression of PROS with TLL suppresses brain hyperplasia (Fig. 7G). Notably, the *cis*-regulatory region of *pros* harbors a consensus TLL binding site within 500 base pairs from the transcriptional initiation site (M. K. and K. F. T., unpublished observations), consistent with the idea that TLL might repress transcription of *pros* via direct DNA binding.

Recently, atypical large Nb lineages in the dorsomedial part of the larval brain have been described and designated as Posterior Asense-Negative (PAN) Nbs (Bello et al., 2008; Bowman et al., 2008; Boone and Doe, 2008). Nbs of such lineages divide asymmetrically to self renew, but, unlike other Nbs, generate smaller intermediate progenitors that express Nb markers. The fact that these atypical Nbs are MIRA-positive and PROS negative raises a possibility that tumor clones induced by TLL could either correspond to or originate from them. As with other Nbs, clones of the PAN-Nb lineages accompany only a single large Nb, with their progeny arranged regularly in a columnar order (Sup. Fig. 6A; Bello et al., 2008;

Bowman et al., 2008; Boone and Doe, 2008). By contrast, clones generated by TLL overexpression harbor several large to intermediate-sized Nbs, exhibiting irregular morphology (Sup. Fig. 6B), which is typical of tumors. Bowman et al. (2008) has also shown that PAN-Nbs are the Nb subpopulation that exhibits overgrowth in *brat* mutants. However, it is also unlikely that TLL induced overgrowth originates from overgrowth of PAN Nbs, which correspond to eight Nbs in the DPM group (Pereanu et al., 2006) among the ~90 Nbs per hemisphere. On the contrary, TLL induces clonal tumors not only in DPM but also in CM and BLP lineages (Fig. 6). Indeed, TLL overgrowth phenotype is not localized to a specific location of the hemisphere, but broadly detectable in the brain including the optic lobe (Fig. 5I and Sup. Fig. 5B). Moreover, TLL overgrowth phenotype is also induced in the embryonic CNS (Sup. Fig. 4), arguing against the involvement of larval PAN-Nbs.

Conserved regulatory mechanism of neural progenitor proliferation by *tll/Tlx* homologs

The *Drosophila* TLL and the vertebrate homolog TLX (NR2E1) share high sequence similarity in the DNA binding domain (Yu et al., 1994; Monaghan et al., 1995). *Tlx* mutant mice exhibit a reduction of rhinencephalon and limbic structures with emotional and learning defects (Monaghan et al., 1997; Roy et al., 2002). Notably, *Tlx* mutant mice exhibit reduction of neuron numbers in cortical upper layers (Roy et al., 2004), which are generated by GMC-like intermediate progenitors (Noctor et al., 2004; Haubensak et al., 2004; Miyata et al., 2004). Postnatally, TLX is localized to the adult neurogenic regions including the subgranular layer of the dentate gyrus to maintain stem cells in a proliferative and undifferentiated state (Monaghan et al., 1997; Shi et al., 2004). Recent behavioral studies have shown that such TLX-positive neural stem cells actually contribute to animal's spatial learning (Zhang et al., 2008). Thus, combined with our results, these studies highlight a

functional commonality of the *tll*/*Tlx* homologs between flies and mammals, and imply an intriguing evolutionary conservation of the genetic programs underlying neural progenitor controls in crucial brain structures involved in memory and other cognitive functions.

Intriguingly, the mammalian *pros* homolog *Prox1* promotes cell cycle exit and differentiation of the neural progenitors in the developing subventricular zone and the retina (Torii et al., 1999; Dyer et al., 2003; Lavado and Oliver, 2007), the neural tissues in that *Tlx* functions antagonistically to control progenitor proliferation (Roy et al., 2004: Shi et al., 2004; Miyawaki et al., 2004; Zhang et al., 2006). Based on the *tll* GOF phenotypes in *Drosophila*, we predict that deregulation of *Tlx* in the developing brain may cause suppression of *Prox1* and could result in severe neurological tumors in humans. On the other hand, consistent with the loss-of-function phenotypes in flies, several mutations have been identified in the regulatory regions of *Tlx* in humans with microcephary (Kumar et al., 2007). Given the commonality in progenitor control, further studies of the *Drosophila* MB-Nbs may shed light on the molecular basis of the proliferation and differentiation of neural progenitors, and would provide important cues for understanding progenitor disorders in the human brain.

Acknowledgements

We thank Drs. F. Matsuzaki, N. Fuse, V. Rodrigues, J. Knoblich, L. Luo, Y. Hiromi, U. Walldorf, J. Lengyel, D. Kosman, C. O'Kane, H. Keshishian, H. Richardson, R. Saint, E. Hafen, and T. Isshiki, as well as the Bloomington Stock Center and Developmental Studies Hybridoma Bank for generous sharing of the fly stocks and antibodies. We also thank members of the Suzuki and Furukubo-Tokunaga labs for helpful discussions and M. Taniguchi for excellent technical assistance. This work was supported by Grants-in-Aid for Scientific Research from MEXT Japan (KFT, MK, ES), Naito Foundation (MK), and by the Tsukuba Advanced Research Alliance (KFT).

References

Adachi, Y., Hauck, B., Clements, J., Kawauchi, H., Kurusu, M., Totani, Y., Kang, Y. Y., Eggert, T., Walldorf, U., Furukubo-Tokunaga, K., Callaerts, P., 2003. Conserved cis-regulatory modules mediate complex neural expression patterns of the eyeless gene in the *Drosophila* brain. Mech. Dev. 120**,** 1113-1126.

Almeida, M. S., Bray, S. J., 2005. Regulation of post-embryonic neuroblasts by *Drosophila* Grainyhead. Mech. Dev. 122**,** 1282-1293.

Alvarez-Buylla, A., Garcia-Verdugo, J. M., Tramontin, A. D., 2001. A unified hypothesis on the lineage of neural stem cells. Nat. Rev. Neurosci. 2**,** 287-293.

Bello, B., Reichert, H., Hirth, F., 2006. The *brain tumor* gene negatively regulates neural progenitor cell proliferation in the larval central brain of *Drosophila*. Development 133**,** 2639-2648.

Bello, B. C., Hirth, F., Gould, A. P., 2003. A pulse of the *Drosophila* Hox protein Abdominal-A schedules the end of neural proliferation via neuroblast apoptosis. Neuron 37**,** 209-219.

Bello, B. C., Izergina, N., Caussinus, E., Reichert, H., 2008. Amplification of neural stem cell proliferation by intermediate progenitor cells in *Drosophila* brain development. Neural Develop. 3**,** 5.

Betschinger, J., Knoblich, J. A., 2004. Dare to be different: asymmetric cell division in *Drosophila, C. elegans* and vertebrates. Curr. Biol. 14**,** R674-685.

Betschinger, J., Mechtler, K., Knoblich, J. A., 2006. Asymmetric segregation of the tumor suppressor *brat* regulates self-renewal in *Drosophila* neural stem cells. Cell 124**,** 1241-1253.

Boone, J. Q., Doe, C. Q., 2008. Identification of *Drosophila* type II neuroblast lineages

containing transit amplifying ganglion mother cells. Dev. Neurobiol. 68**,** 1185-1195.

Bowman, S. K., Rolland, V., Betschinger, J., Kinsey, K. A., Emery, G., Knoblich, J. A., 2008. The tumor suppressors Brat and Numb regulate transit-amplifying neuroblast lineages in *Drosophila*. Dev. Cell 14**,** 535-546.

Callaerts, P., Leng, S., Clements, J., Benassayag, C., Cribbs, D., Kang, Y. Y., Walldorf, U., Fischbach, K. F., Strauss, R., 2001. *Drosophila* Pax-6/*eyeless* is essential for normal adult brain structure and function. J. Neurobiol. 46**,** 73-88.

Caussinus, E., Gonzalez, C., 2005. Induction of tumor growth by altered stem-cell asymmetric division in *Drosophila melanogaster*. Nat. Genet. 37**,** 1125-1129.

Cayre, M., Strambi, C., Strambi, A., 1994. Neurogenesis in an adult insect brain and its hormonal control. Nature 368**,** 57-59.

Cenci, C., Gould, A. P., 2005. *Drosophila* Grainyhead specifies late programmes of neural proliferation by regulating the mitotic activity and Hox-dependent apoptosis of neuroblasts. Development 132**,** 3835-3845.

Chia, W., Somers, W. G., Wang, H., 2008. *Drosophila* neuroblast asymmetric divisions: cell cycle regulators, asymmetric protein localization, and tumorigenesis. J. Cell Biol. 180**,** 267-272.

Choksi, S. P., Southall, T. D., Bossing, T., Edoff, K., de Wit, E., Fischer, B. E., van Steensel, B., Micklem, G., Brand, A. H., 2006. Prospero acts as a binary switch between self-renewal and differentiation in *Drosophila* neural stem cells. Dev. Cell 11**,** 775-789.

Connolly, J. B., Roberts, I. J., Armstrong, J. D., Kaiser, K., Forte, M., Tully, T., O'Kane, C. J., 1996. Associative learning disrupted by impaired Gs signaling in *Drosophila* mushroom bodies. Science 274**,** 2104-2107.

Doe, C. Q., 2008. Neural stem cells: balancing self-renewal with differentiation. Development 135**,** 1575-1587.

Dufour, M. C., Gadenne, C., 2006. Adult neurogenesis in a moth brain. J. Comp. Neurol. 495**,** 635-643.

Dumstrei, K., Wang, F., Hartenstein, V., 2003. Role of DE-cadherin in neuroblast proliferation, neural morphogenesis, and axon tract formation in *Drosophila* larval brain development. J. Neurosci. 23**,** 3325-3335.

Dyer, M. A., Livesey, F. J., Cepko, C. L., Oliver, G., 2003. Prox1 function controls progenitor cell proliferation and horizontal cell genesis in the mammalian retina. Nat. Genet. 34**,** 53-58.

Gage, F. H., 2000. Mammalian neural stem cells. Science 287**,** 1433-1438.

Haubensak, W., Attardo, A., Denk, W., Huttner, W. B., 2004. Neurons arise in the basal neuroepithelium of the early mammalian telencephalon: a major site of neurogenesis. Proc. Natl. Acad. Sci. U. S. A. 101**,** 3196-3201.

Hevner, R. F., 2006. From radial glia to pyramidal-projection neuron: transcription factor cascades in cerebral cortex development. Mol. Neurobiol. 33**,** 33-50.

Ikeshima-Kataoka, H., Skeath, J. B., Nabeshima, Y., Doe, C. Q., Matsuzaki, F., 1997. Miranda directs Prospero to a daughter cell during *Drosophila* asymmetric divisions. Nature 390**,** 625-629.

Isshiki, T., Pearson, B., Holbrook, S., Doe, C. Q., 2001. *Drosophila* neuroblasts sequentially express transcription factors which specify the temporal identity of their neuronal progeny. Cell 106**,** 511-521.

Ito, K., Awano, W., Suzuki, K., Hiromi, Y., Yamamoto, D., 1997. The *Drosophila* mushroom body is a quadruple structure of clonal units each of which contains a virtually

identical set of neurons and glial cells. Development 124**,** 761-771.

Ito, K., Hotta, Y., 1992. Proliferation pattern of postembryonic neuroblasts in the brain of *Drosophila melanogaster*. Dev. Biol. 149**,** 134-148.

Izumi, Y., Ohta, N., Hisata, K., Raabe, T., Matsuzaki, F., 2006. *Drosophila* Pins-binding protein Mud regulates spindle-polarity coupling and centrosome organization. Nat. Cell Biol. 8**,** 586-593.

Jefferis, G. S., Marin, E. C., Stocker, R. F., Luo, L., 2001. Target neuron prespecification in the olfactory map of *Drosophila*. Nature 414**,** 204-208.

Kosman, D., Small, S., Reinitz, J., 1998. Rapid preparation of a panel of polyclonal antibodies to *Drosophila* segmentation proteins. Dev. Genes Evol. 208**,** 290-294.

Kumar, R. A., Leach, S., Bonaguro, R., Chen, J., Yokom, D. W., Abrahams, B. S., Seaver, L., Schwartz, C. E., Dobyns, W., Brooks-Wilson, A., Simpson, E. M., 2007. Mutation and evolutionary analyses identify NR2E1-candidate-regulatory mutations in humans with severe cortical malformations. Genes Brain Behav. 6**,** 503-516.

Kurusu, M., Awasaki, T., Masuda-Nakagawa, L. M., Kawauchi, H., Ito, K., Furukubo-Tokunaga, K., 2002. Embryonic and larval development of the *Drosophila* mushroom bodies: concentric layer subdivisions and the role of *Fasciclin II*. Development 129**,** 409-419.

Kurusu, M., Nagao, T., Walldorf, U., Flister, S., Gehring, W. J., Furukubo-Tokunaga, K., 2000. Genetic control of development of the mushroom bodies, the associative learning centers in the *Drosophila* brain by the eyeless, twin of eyeless, and Dachshund genes. Proc. Natl. Acad. Sci. U. S. A. 97**,** 2140-2144.

Lavado, A., Oliver, G., 2007. *Prox1* expression patterns in the developing and adult murine brain. Dev. Dyn. 236**,** 518-524.

Lee, C. Y., Robinson, K. J., Doe, C. Q., 2006a. Lgl, Pins and aPKC regulate neuroblast self-renewal versus differentiation. Nature 439**,** 594-598.

Lee, C. Y., Wilkinson, B. D., Siegrist, S. E., Wharton, R. P., Doe, C. Q., 2006b. Brat is a Miranda cargo protein that promotes neuronal differentiation and inhibits neuroblast self-renewal. Dev. Cell 10**,** 441-449.

Lee, T., Luo, L., 1999. Mosaic analysis with a repressible cell marker for studies of gene function in neuronal morphogenesis. Neuron 22**,** 451-461.

Luo, L., Liao, Y. J., Jan, L. Y., Jan, Y. N., 1994. Distinct morphogenetic functions of similar small GTPases: *Drosophila* Drac1 is involved in axonal outgrowth and myoblast fusion. Genes Dev. 8**,** 1787-1802.

Mardon, G., Solomon, N. M., Rubin, G. M., 1994. *dachshund* encodes a nuclear protein required for normal eye and leg development in *Drosophila*. Development 120**,** 3473-3486.

Martini, S. R., Roman, G., Meuser, S., Mardon, G., Davis, R. L., 2000. The retinal determination gene, *dachshund*, is required for mushroom body cell differentiation. Development 127**,** 2663-2672.

Maurange, C., Cheng, L., Gould, A. P., 2008. Temporal transcription factors and their targets schedule the end of neural proliferation in *Drosophila*. Cell 133**,** 891-902.

Maurange, C., Gould, A. P., 2005. Brainy but not too brainy: starting and stopping neuroblast divisions in *Drosophila*. Trends Neurosci. 28**,** 30-36.

Ming, G. L., Song, H., 2005. Adult neurogenesis in the mammalian central nervous system. Annu. Rev. Neurosci. 28**,** 223-250.

Miyata, T., Kawaguchi, A., Saito, K., Kawano, M., Muto, T., Ogawa, M., 2004. Asymmetric production of surface-dividing and non-surface-dividing cortical progenitor cells.

Development 131**,** 3133-3145.

Miyawaki, T., Uemura, A., Dezawa, M., Yu, R. T., Ide, C., Nishikawa, S., Honda, Y., Tanabe, Y., Tanabe, T., 2004. Tlx, an orphan nuclear receptor, regulates cell numbers and astrocyte development in the developing retina. J. Neurosci. 24**,** 8124-8134.

Monaghan, A. P., Bock, D., Gass, P., Schwager, A., Wolfer, D. P., Lipp, H. P., Schutz, G., 1997. Defective limbic system in mice lacking the *tailless* gene. Nature 390**,** 515-517.

Monaghan, A. P., Grau, E., Bock, D., Schutz, G., 1995. The mouse homolog of the orphan nuclear receptor *tailless* is expressed in the developing forebrain. Development 121**,** 839-853.

Moran, E., Jimenez, G., 2006. The *tailless* nuclear receptor acts as a dedicated repressor in the early *Drosophila* embryo. Mol. Cell Biol. 26**,** 3446-3454.

Noctor, S. C., Martinez-Cerdeno, V., Ivic, L., Kriegstein, A. R., 2004. Cortical neurons arise in symmetric and asymmetric division zones and migrate through specific phases. Nat. Neurosci. 7**,** 136-144.

Noctor, S. C., Martinez-Cerdeno, V., Kriegstein, A. R., 2007. Contribution of intermediate progenitor cells to cortical histogenesis. Arch. Neurol. 64**,** 639-642.

Noveen, A., Daniel, A., Hartenstein, V., 2000. Early development of the *Drosophila* mushroom body: the roles of *eyeless* and *dachshund*. Development 127**,** 3475-3488.

Osterwalder, T., Yoon, K. S., White, B. H., Keshishian, H., 2001. A conditional tissue-specific transgene expression system using inducible GAL4. Proc. Natl. Acad. Sci. U. S. A. 98**,** 12596-12601.

Pearson, B. J., Doe, C. Q., 2003. Regulation of neuroblast competence in *Drosophila*. Nature 425**,** 624-628.

Pereanu, W., Hartenstein, V., 2006. Neural lineages of the *Drosophila* brain: a

three-dimensional digital atlas of the pattern of lineage location and projection at the late larval stage. J. Neurosci. 26**,** 5534-5553.

Pignoni, F., Baldarelli, R. M., Steingrimsson, E., Diaz, R. J., Patapoutian, A., Merriam, J. R., Lengyel, J. A., 1990. The *Drosophila* gene *tailless* is expressed at the embryonic termini and is a member of the steroid receptor superfamily. Cell 62**,** 151-163.

Reddy, G. V., Rodrigues, V., 1999. Sibling cell fate in the *Drosophila* adult external sense organ lineage is specified by prospero function, which is regulated by Numb and Notch. Development 126**,** 2083-2092.

Richardson, H., O'Keefe, L. V., Marty, T., Saint, R., 1995. Ectopic cyclin E expression induces premature entry into S phase and disrupts pattern formation in the *Drosophila* eye imaginal disc. Development. 121**,** 3371-3379.

Richardson, H. E., O'Keefe, L. V., Reed, S. I., Saint, R., 1993. A *Drosophila* G1-specific cyclin E homolog exhibits different modes of expression during embryogenesis. Development 119**,** 673-690.

Rolls, M. M., Albertson, R., Shih, H. P., Lee, C. Y., Doe, C. Q., 2003. *Drosophila* aPKC regulates cell polarity and cell proliferation in neuroblasts and epithelia. J. Cell Biol. 163**,** 1089-1098.

Roy, K., Kuznicki, K., Wu, Q., Sun, Z., Bock, D., Schutz, G., Vranich, N., Monaghan, A. P., 2004. The *Tlx* gene regulates the timing of neurogenesis in the cortex. J. Neurosci. 24**,** 8333-8345.

Roy, K., Thiels, E., Monaghan, A. P., 2002. Loss of the *tailless* gene affects forebrain development and emotional behavior. Physiol. Behav. 77**,** 595-600.

Shi, Y., Chichung Lie, D., Taupin, P., Nakashima, K., Ray, J., Yu, R. T., Gage, F. H., Evans, R. M., 2004. Expression and function of orphan nuclear receptor TLX in adult neural

stem cells. Nature 427**,** 78-83.

Technau, G., Heisenberg, M., 1982. Neural reorganization during metamorphosis of the corpora pedunculata in *Drosophila melanogaster*. Nature 295**,** 405-407.

Tettamanti, M., Armstrong, J. D., Endo, K., Yang, M. Y., Furukubo-Tokunaga, K., Kaiser, K., Reichert, H., 1997. Early development of the *Drosophila* mushroom bodies, brain centres for associative learning and memory. Dev. Genes Evol. 207**,** 242-252.

Torii, M., Matsuzaki, F., Osumi, N., Kaibuchi, K., Nakamura, S., Casarosa, S., Guillemot, F., Nakafuku, M., 1999. Transcription factors Mash-1 and Prox-1 delineate early steps in differentiation of neural stem cells in the developing central nervous system. Development 126**,** 443-456.

Truman, J. W., Bate, M., 1988. Spatial and temporal patterns of neurogenesis in the central nervous system of *Drosophila melanogaster*. Dev. Biol. 125**,** 145-157.

Urbach, R., Technau, G. M., 2003. Molecular markers for identified neuroblasts in the developing brain of *Drosophila*. Development 130**,** 3621-3637.

Younossi-Hartenstein, A., Green, P., Liaw, G. J., Rudolph, K., Lengyel, J., Hartenstein, V., 1997. Control of early neurogenesis of the *Drosophila* brain by the head gap genes *tll*, *otd*, *ems*, and *btd*. Dev. Biol. 182**,** 270-283.

Younossi-Hartenstein, A., Nguyen, B., Shy, D., Hartenstein, V., 2006. Embryonic origin of the *Drosophila* brain neuropile. J. Comp. Neurol. 497**,** 981-998.

Yu, F., Kuo, C. T., Jan, Y. N., 2006. *Drosophila* neuroblast asymmetric cell division: recent advances and implications for stem cell biology. Neuron 51**,** 13-20.

Yu, R. T., McKeown, M., Evans, R. M., Umesono, K., 1994. Relationship between *Drosophila* gap gene tailless and a vertebrate nuclear receptor Tlx. Nature 370**,** 375-379.

Zhang, C. L., Zou, Y., He, W., Gage, F. H., Evans, R. M., 2008. A role for adult TLX-positive neural stem cells in learning and behaviour. Nature 451**,** 1004-1007.

Zhang, C. L., Zou, Y., Yu, R. T., Gage, F. H., Evans, R. M., 2006. Nuclear receptor TLX prevents retinal dystrophy and recruits the corepressor atrophin1. Genes. Dev. 20**,** 1308-1320.

Zhu, S., Lin, S., Kao, C. F., Awasaki, T., Chiang, A. S., Lee, T., 2006. Gradients of the *Drosophila* Chinmo BTB-zinc finger protein govern neuronal temporal identity. Cell 127**,** 409-422.

Figure legends

Figure 1. TLL is expressed in MB neuroblasts and GMCs.

(A) A diagram showing the proliferation patterns of the *Drosophila* brain Nbs. L1, L2 and L3; first, second and third instar larval stages. (B and B1) Expression of TLL in the embryonic brain at late stage 16. Triple labeling with anti-TLL (magenta), anti-DAC (blue), and a pan-neural maker, anti-HRP antibody (green). Dorsal view. Arrows, MB primordia. (C) TLL (magenta) and DAC (green) in the first instar larval brain. (D) TLL in the third instar brain. Open arrowheads, lamina precursor cells. (E) TLL and DAC in MB neurons at the third instar stage. (F-H) TLL expression in the pupal brain at 20h APF (F) and 50h APF (G, H). (I) TLL in the adult MB at several hours after eclosion. In (D and F-I), MBs are labeled with OK107 > *UAS-mCD8::GFP* (green). Scale bars: 25 μm in (B); 15 μm in (C); 50 μm in (D); 25 μm in (E); 50 μm in (F), applies also to (G); and 25 μm in (H), applies also to (I). Arrows, MB-Nbs. Arrowheads, MB-GMCs.

Figure 2. Mutation of *tll* leads to significant reduction in MB clone size.

(A-C) Third instar MB-Nb clones generated by MARCM. (D and E) Adult MB-Nb clones (green). Double staining with anti-FAS II (magenta), which labels the α/β lobes and weakly labels the γ lobe. (F) Rescue of the tll^{1} MB-Nb clone with *UAS-tll*. Third instar stage. Number of neurons is indicated in each panel. Abbreviations: CX, calyx; DL, dorsal lobe; ML, medial lobe. MBs are labeled with *UAS-mCD8::GFP* driven by OK107 in (A and C-E) or by *elav-Gal4*^{c155} in (B and F). Mitotic recombination was induced at the early first instar stage. Scale bars: 25 μm in (A), applies also to (B, C, and F); 25 μm in (D), applies also to (E).

Figure 3. Loss of *tll* function progressively impairs cell cycle in MB-Nbs and causes premature loss of MB-Nbs in the early pupal stage.

(A and B) MB-Nbs in wild-type (A) and tll^{l49} mutant clones (B) at the third instar and the pupal stages. Arrows, MB-Nbs; arrowheads, MB-GMCs. Number of clones accompanying an identifiable Nb is indicated. Dividing cells were labeled with BrdU (magenta). Note that, although MB mutant clones retained identifiable Nbs at 20 h APF, many of them were not mitotically active lacking BrdU incorporation. (C) Fractions of Nbs labeled with BrdU or anti-PH3. Number of each sample is indicated in the bar. Only sample numbers are indicated for mutant clones of 40 h and 60 h APF because they lacked identifiable Nbs. (D-K) Cyc E and Cyc B expression (magenta) in wild-type and tll^{l49} mutant clones at the third instar stage (D-G) and 20 h APF (H-K). Arrows, MB-Nbs. Mutant clones were induced at the early first instar stage. (L) Fractions of Nbs labeled with anti-Cyc E or anti-Cyc B at the third instar stage and 20 h APF. Number of each sample is indicated in the bar. MBs are labeled with *UAS-mCD8::GFP* (green) driven by OK107 (green). Mutant clones were induced at the early first instar stage. Scale bar: 10 μm in (A), applies also to (B); 10 μm in (D), applies also to (E-G); 10 μm in (H), applies also to (I-K).

Figure 4. Loss of *tll* function causes cell cycle defects and apoptosis in MB-GMCs.

(A) Cell cycle activity in wild-type and tll^{l49} mutant MB-GMCs. Number of each sample is indicated in the bar. BrdU labeling was performed for 1 h immediately after dissection. Note the significant suppression of cell division activity in *tll* mutant MB-GMCs. (B-E) BrdU pulse-chase experiments. MB clones were induced at the early first instar stage. At the early third instar stage, larvae were fed with BrdU-containing food for 3 h, and then dissected immediately (B and D) or after 32 h chase with normal food (C and E). Asterisks,

MB-Nbs. Arrowheads, GMCs. Open arrowheads in (E) indicate nearby wild-type MB neurons labeled with BrdU but not with GFP, the clonal marker. Magenta, BrdU incorporation. Clones are marked with *UAS-mCD8::GFP* driven by OK107 (green). Blue, MB cells labeled with anti-EY antibody. Scale bars: 10 μm. (F) Number of BrdU labeled GMC and neurons per clone before and after chase. (G-J) Apoptotic cells in wild-type and tll^{l49} mutant clones at the third instar stage (L3) and 20 h APF. Magenta, TUNEL positive cells. Note the apoptotic signals in mutant MB-GMCs (arrowheads in I and J). No TUNEL signals were found for Nb and neurons. MB cells are marked by *UAS-mCD8::GFP* (green) driven by *elav-Gal4* (G and H) or OK107 (I and J). Scale bar, 10 μm. (K) Number of TUNEL positive cells per clone at the third instar stage (L3) and 20 h APF. In (F and K), number of each sample is indicated in the bar. $^{**}p<0.01$ with Student's t-test.

Figure 5. Brain hyperplasia caused by ectopic TLL expression.

(A) Quantitative analysis of BrdU incorporation in wild-type and *tll* GOF brains. Note that overexpression of TLL stimulates cell division in the larval and pupal brains. CB, central brain. OL, optic lobes. Total number of pixels for BrdU signals was calculated with an image analysis program based on Z-series of optical sections covering the entire brain hemisphere. $^{*}p<0.05$ and $^{**}p<0.01$ with Student's t-test. Number of each sample is indicated in the bar. Ectopic expression of *tll* was induced by *elav-GeneSwitch*. Newly molted third instar larvae were fed with RU486 food and dissected at the late third instar stage or 40 h APF. (B-G) Higher magnification views of wild-type and *tll* GOF brains. Larval brains were double labeled for the indicated cell cycle markers (BrdU, Cyc B, Cyc E and PH3). Confocal sections of corresponding focal planes. Third instar stage. Arrowheads indicate wild-type Nbs (B-D) or intermediate-sized Nb-like cells (E-G). Note the

supernumerary Nbs in *tll* GOF brain. Scale bar: 10 μm. (H and I) Expression of MIRA (magenta) and PROS (blue) in wild-type and *tll* GOF brains. Confocal sections of corresponding focal planes. Note the densely and irregularly packed MIRA positive cells in the central brain of the *tll* GOF larvae at the expense of PROS positive cells. Third instar stage. Scale bar: 20 μm. (J) Number of MIRA positive cells per brain hemisphere. Large to intermediate-sized Nb-like cells (the major axis > 6 μm) were counted based on the confocal sections of corresponding focal planes. Third instar stage. Number of each sample is indicated in the bar. $^{**}p<0.01$ with Student's t-test.

Figure 6. TLL overexpression generates supernumerary-Nb clones.

(A) A schematic Nb lineage map in the larval brain. Groupings of the Nb lineages are according to Pereanu et al. (2006). (B) Number of Nbs per wild-type and *tll* mutant clone of the indicated lineage group. Large to intermediate-sized Nb-like cells with the major diameters > 6 μm were counted for each clone. $^{*}p<0.05$ and $^{**}p<0.01$ with Student's t-test. Number of each sample is indicated in the bar. (C-F) Wild-type and *tll* GOF clones of the indicated Nb lineages. Clones were induced at the first instar. *UAS-tll* was driven by *elav-Gal4* with *UAS-mCD8::GFP* (green). MIRA (magenta) and PROS (blue). Asterisks indicate wild-type Nbs (C and E) or PROS- and MIRA+ Nb-like cells (the major axis > 6 μm) (D and F). Arrowheads in (C and E) indicate GMCs expressing PROS. Dotted lines demarcate the outline of the clones. Scale bar: 10 μm in (C), also applies to (D-F).

Figure 7. Distinctive requirements of *pros* and *tll* in MB- and non-Mb progenitors.

(A) Expression of TLL (magenta) and PROS (blue) in the wild-type MB. Third instar. Note the coexpression of TLL and PROS in the MB-GMCs (arrowhead), but not in the

MB-Nb (arrow). (B) PROS expression is not altered in *tll* mutant MB clones. Third instar. PROS (blue) and MIRA (magenta). For wild-type control, see Sup. Fig. 7C. (C and D) Clonal phenotypes of tll^{149} and $pros^{17}$ double mutants in MB and non-MB lineages. (C) MB-Nb clone and (D) non-MB Nb clone. Blue, DAC expression. Numbers of reduced MB clones (C) or tumor clones (D) are indicated. Arrows, MB-Nb. Arrowheads, MB-GMCs. Asterisks in (D) indicate multiple Nbs. In (A-D), cells were labeled with OK107 > *UAS-mCD8:: GFP*. Clones were induced at the first instar. (E-G) Suppression of TLL-induced brain hyperplasia by PROS coexpression. Brain hemispheres at third instar stage. Note the restoration of the wild-type Nb pattern in the *tll pros* GOF brain (G). Nbs were visualized with anti-MIRA. Overexpression was induced by *elav-GeneSwitch* with RU486 fed from newly molted third instar larvae. OL, optic lobe. CB, central brain. Scale bars: 20 μm except for (B), 10 μm.

Supplementary Figure 1. Proliferation pattern of the *Drosophila* MB-Nbs.

(A) Embryonic stage 16. Dorsal view. (B) Early first instar stage. (C and D) Late third instar stage. (D) Higher magnification image showing the Nbs (arrows). (E-G) Pupal stages of the indicated time. (H) Newly eclosed adult. Green, *UAS-mCD8::GFP* driven by the indicated driver. Proliferating cells are marked with BrdU (magenta) or anti-PH3 (blue). CB, central brain. OL, optic lobe. Scale bars: 40 μm in (A); 20 μm in (B and C); 10 μm in (D); 50 μm in (E), applies also to (F and G); and 50 μm in (H). Arrows in (A, B, and E-G) indicate the MB-Nbs.

Supplementary Figure 2. Mutation of *tll* dose not alter the expression of EY and DAC in the MBs.

(A-C) Expression of EY in wild-type (A) and *tll*^{l49} (B and C) clones in the third instar larval brain. Cells are labeled with *UAS-mCD8::GFP* (green) driven by OK107. Asterisks, MB-Nbs. Note EY is normally expressed in the mutant Nb (asterisk in B), GMC (arrow head) and neurons (open arrowhead in C). (D and E) Expression of DAC in wild-type (D) and *tll*^{l49} (E) clones in the third instar larval brain. Although the number of neurons is much reduced in the mutant, DAC is expressed in the mutant neurons (open arrowhead in C). (F-H) TLL expression in the embryonic MB primordia. Neurons are visualized with anti-HRP staining (green). Asterisks, MB-Nbs. Note neither *ey* nor *dac* mutation abolished TLL expression. Scale bars: 10 μm in (A-E); 10 μm in (F), applies also to (G and H).

Supplementary Figure 3. Expression of p35 fails to rescue MB defects in *tll* mutant clones.

(A) Wild-type MB. (B) *tll*^{l49} mutant MB clone. (C) *tll*^{l49} mutant MB clone with p35 expression. 40 h APF. Clones are marked with *UAS-mCD8::GFP* (green) driven by OK107 along with *UAS-p35*. A and B are same images as in Fig. 3A and B for comparison. Scale bars: 10 μm in (A), applies also to (B); 10 μm in (C).

Supplementary Figure 4. Embryonic CNS hyperplasia caused by TLL overexpression.

(A-D) Embryonic CNS hyperplasia at the stage 17. (A and B) Wild-type embryos. (C and D) *tll* GOF embryos. CNS expression of *UAS-tll* was driven by *elav-Gal4*. (E-H) Cell division activities in *tll* GOF CNS at the embryonic stage 16. (E and F) Control. (G and H) *tll* GOF CNS. Embryos were double labeled for BrdU (magenta) and anti-PH3 (blue). (A, C, E, and G) Dorsal views of the embryonic brain. (B, D, F, and H) Ventral ganglia of

the same embryos. Neural cells are visualized with *UAS-mCD8::GFP* (green) under *elav-Gal4*. Scale bars: 40 μm (A) and 100 μm (B).

Supplementary Figure 5. Overexpression of TLL causes aberrant mitotic activity in the larval and pupal brains.

(A and B) Brain hemispheres of wild-type and *tll* GOF larvae. Third instar stage. Magenta, BrdU; blue, anti-PH3. Confocal sections of the corresponding focal planes. Scale bar: 20 μm. (C and D) Higher magnification views of wild-type and *tll* GOF brains. Third instar stage. MIRA (magenta) and PROS (blue). Confocal sections of corresponding focal planes. Scale bar: 10 μm. Arrowheads indicate wild-type Nbs (C) or intermediate-sized Nb-like cells (D). Newly molted third instar larvae were fed with RU486 food and dissected at the late third instar stage. (E-H) Dividing cells in wild-type and *tll* GOF brains at 40 h APF. Scale bars: 100 μm (E) and 10 μm (F). Arrows in (H) indicate intermediate-sized Nb-like cells. Expression of *tll* was driven by *elav-GeneSwitch*. Newly molted third instar larvae were fed with RU486 food and dissected at 40 h APF. Note persistent *GeneSwitch-Gal4* activity in the pupal stage as revealed by mCD8::GFP expression.

Supplementary Figure 6. Morphological comparison of TLL-induced tumor clone with PAN-Nb and CM-Nb clones.

(A) Large wild-type PAN-Nb clone of the DPM lineages. Arrow indicates the single Nb of the wild-type large clone. (B) Tumor clone of the DPM lineage induced by *tll* overexpression. Arrows, supernumerary Nbs. Note the multiple Nbs and the irregular morphology of the *tll* GOF clone. (C and D) Wild-type Nb clone (C) and a tumor clone (D) in CM lineage. Arrows, Nbs. *UAS-tll* was driven by *elav-Gal4* with *UAS-mCD8::GFP*.

Clones were induced at the first instar. Scale bar: 10 μm, applies also to (B-D).

Supplementary Figure 7. TLL overexpression does not induce supernumerary-Nb clones in the DPL and MB lineages.

(A-D) Wild-type and *tll* GOF clones of the DPL (A and B) and MB (C and D) lineages. Clones were induced at the first instar. *UAS-tll* was driven by *elav-Gal4* with *UAS-mCD8::GFP* (green). MIRA (magenta) and PROS (blue). Asterisks indicate the single Nb in the clone. Arrowheads indicate GMCs expressing PROS. Scale bar: 10 μm in (A), applies also to (B-D).

Supplementary Figure 8. Overexpression of TLL dose not alter the asymmetric localization of aPKC, PINS, and BRAT.

(A and C) Wild-type Nbs. (B and D) *tll* GOF Nbs. Nbs of the CM lineages at the third instar stage. Note that expression and localization of aPKC, PINS, BRAT, and MIRA are not altered in *tll* GOF clones. PROS is expressed in the wild-type GMCs (arrowheads in C) but not in the *tll* GOF GMCs (arrowheads in D). *UAS-tll* and *UAS-mCD8::GFP* were driven by *elav-GeneSwitch* with RU486 fed from newly molted third instar larvae. Scale bars: 5 μm.

Supplementary Figure 9. Distinctive phenotypes of *pros* LOF mutation in MB and non-MB clones.

(A and B) Wild-type MB-Nb clone (A) and non-MB Nb clone (B). Arrows indicate the MB-Nb. (C) $pros^{17}$ non-MB clone harboring multiple Nbs (asterisks). (D) $pros^{17}$ MB clone with a single Nb (arrow). Number of multiple (C) or single (D) Nb clones is indicated. Cellular markers: anti-MIRA (magenta) for Nbs and anti-DAC (blue) for postmitotic neurons.

(E) *pros*^{17} mutant clone of non-MB lineage. Asterisks indicate multiple Nbs typical for *pros* mutant clones. Note that TLL is not upregulated in *pros* mutant clones. (F) *pros*^{17} mutant clone of MB lineage. Arrow, Nb. Arrowhead, GMCs. Note wild-type like TLL expression in the MB-Nb and GMCs. Cells were labeled with OK107 > *UAS-mCD8:: GFP.* Scale bars:10 μm in (A), applies also to (B); 20 μm in (C-F).

Supplementary Figure 10. PROS is not recruited at cell-cycle exit of MB-Nbs.

(A and B) Wild-type MBs at 88 h APF. (A) TLL (blue) and PROS (magenta) expression. (B) MIRA, PH3 (blue) and PROS (magenta) expression. Arrows, MB-Nb. Arrowheads, MB-GMCs. Note PROS is not recruited in the MB-Nb that remains at this stage. Similar results were obtained at 92h APF. Scale bar: 10 μm in (A) applies also to (B). (C) Number of MB-Nbs per brain hemisphere at the end of the pupal stage. Note only one MB-Nb remained identifiable at 88h APF and most MB-Nbs disappeared by 92 h APF. Number of each sample is indicated in the bar.

Supplementary Figure 11. Overexpression of *pros* causes partial loss of MB-Nbs.

(A and B) Wild-type (A) and *pros* GOF (B) MBs at third instar stage. Note the marked reduction in the number of neurons in *pros* GOF MBs. Cells were labeled with OK107 > *UAS-mCD8::GFP.* DL, dorsal lobe. ML, medial lobe. KCs, Kenyon cells. Scale bars: 20 μm. (C) Number of Nbs in wild-type and *pros* GOF MBs. $^{**}p<0.01$ with Student's t-test. Number of each sample is indicated in the bar. *UAS-pros* was driven in MBs by OK107.

Figure 1

Click here to download high resolution image

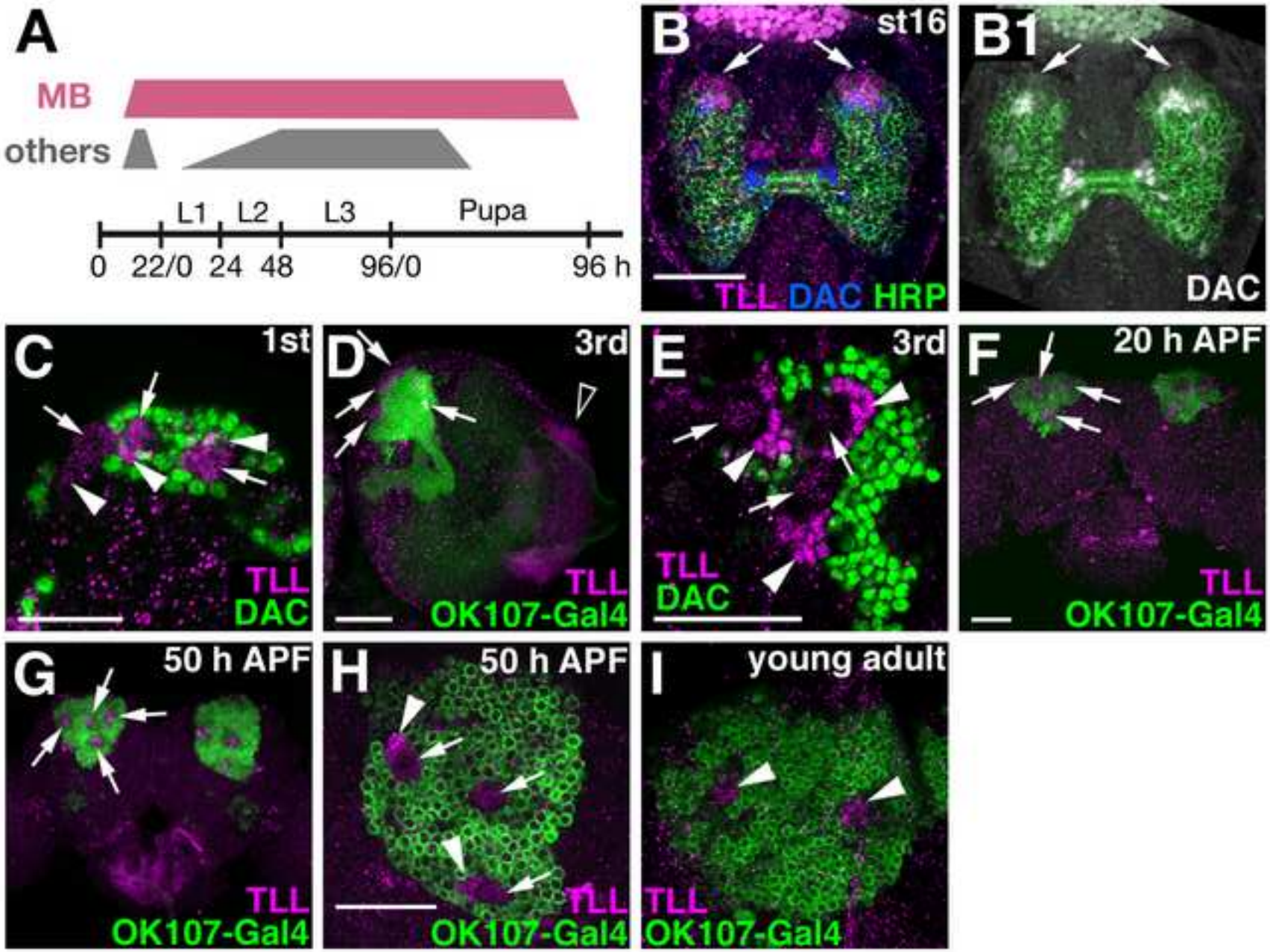

kurusu_Fig. 1

Figure 2

Click here to download high resolution image

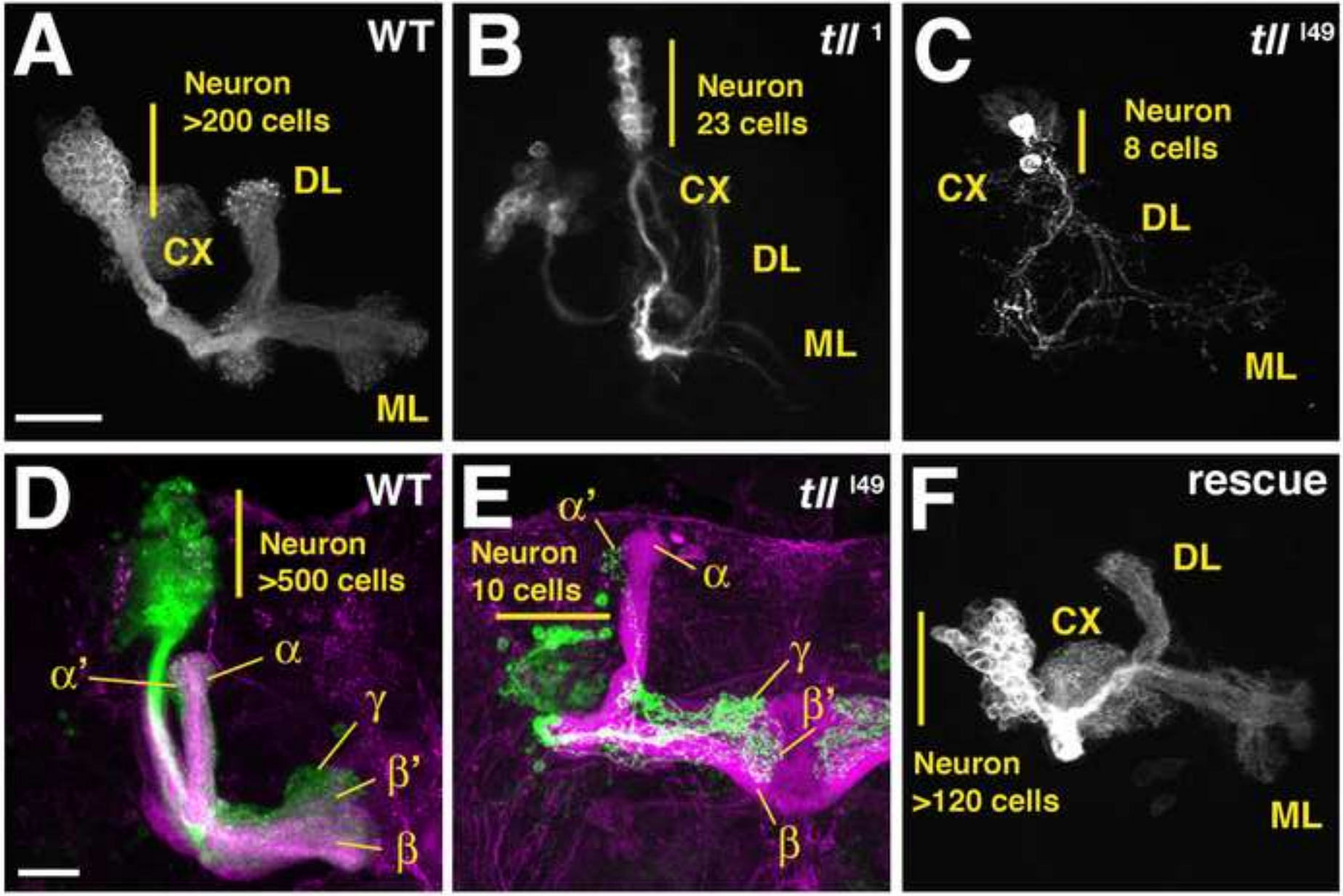

kurusu_Fig. 2

Figure 3

Click here to download high resolution image

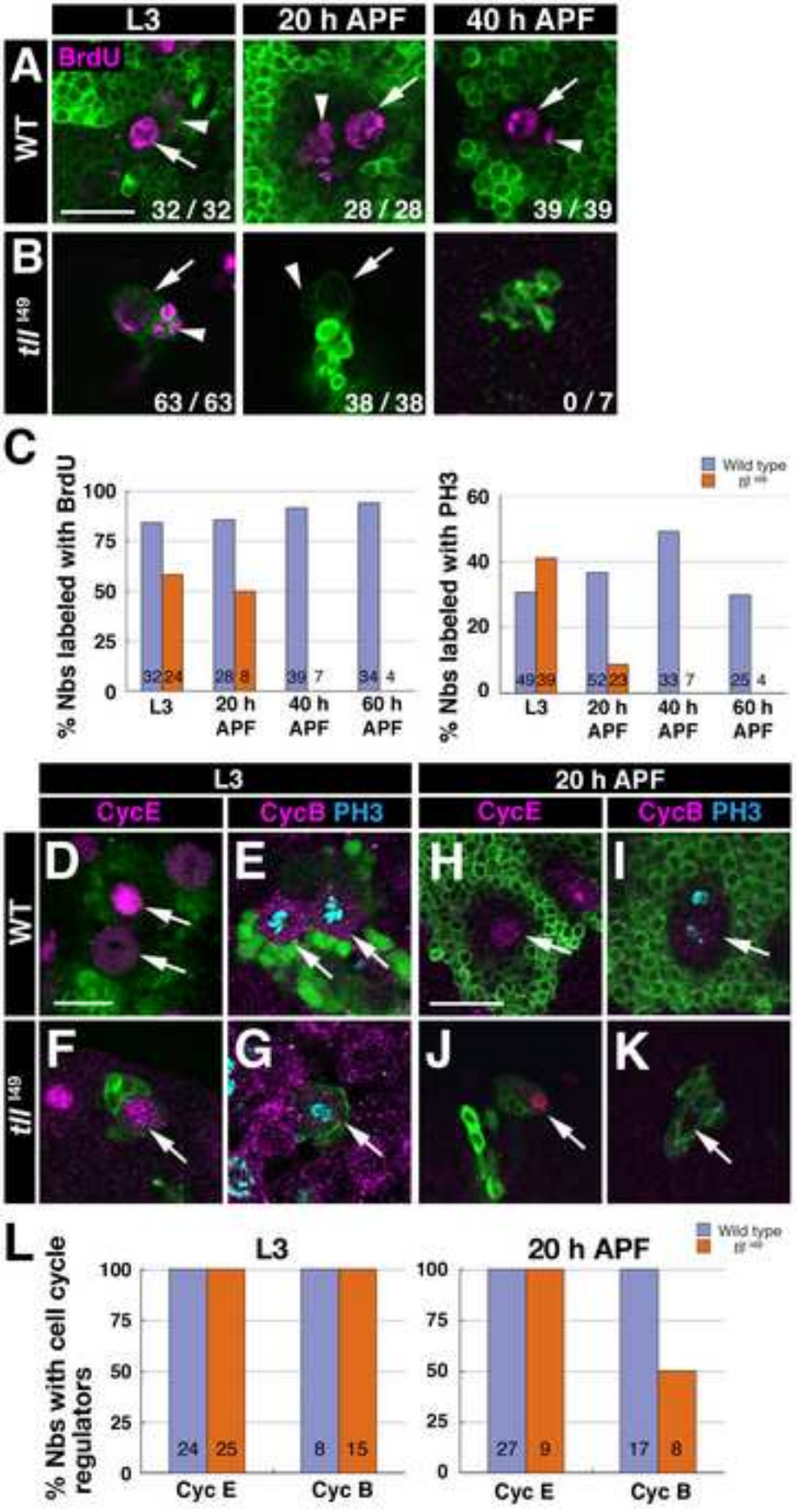

kurusu_Fig. 3

Figure 4

Click here to download high resolution image

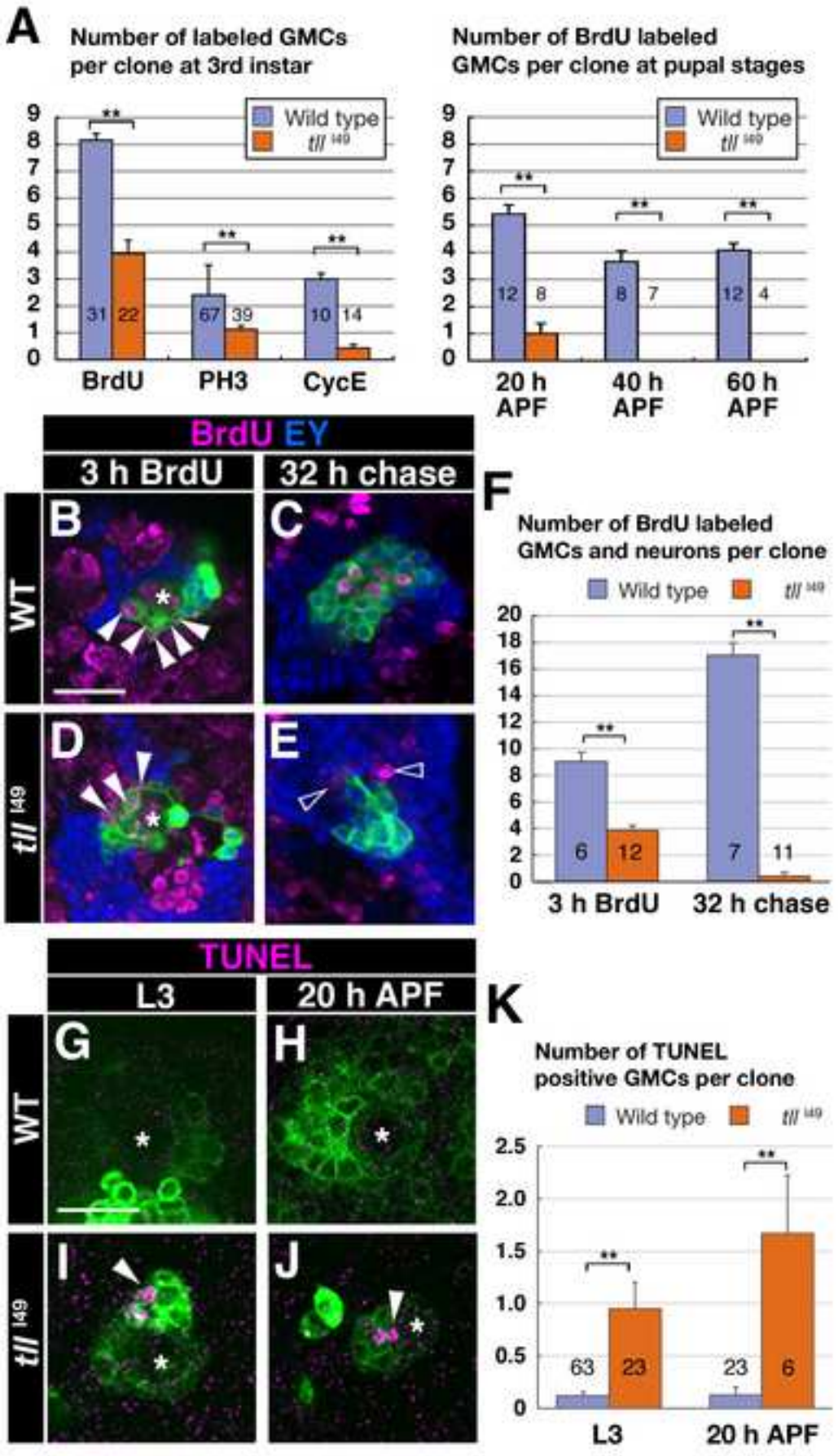

kurusu_Fig. 4

Figure 5

Click here to download high resolution image

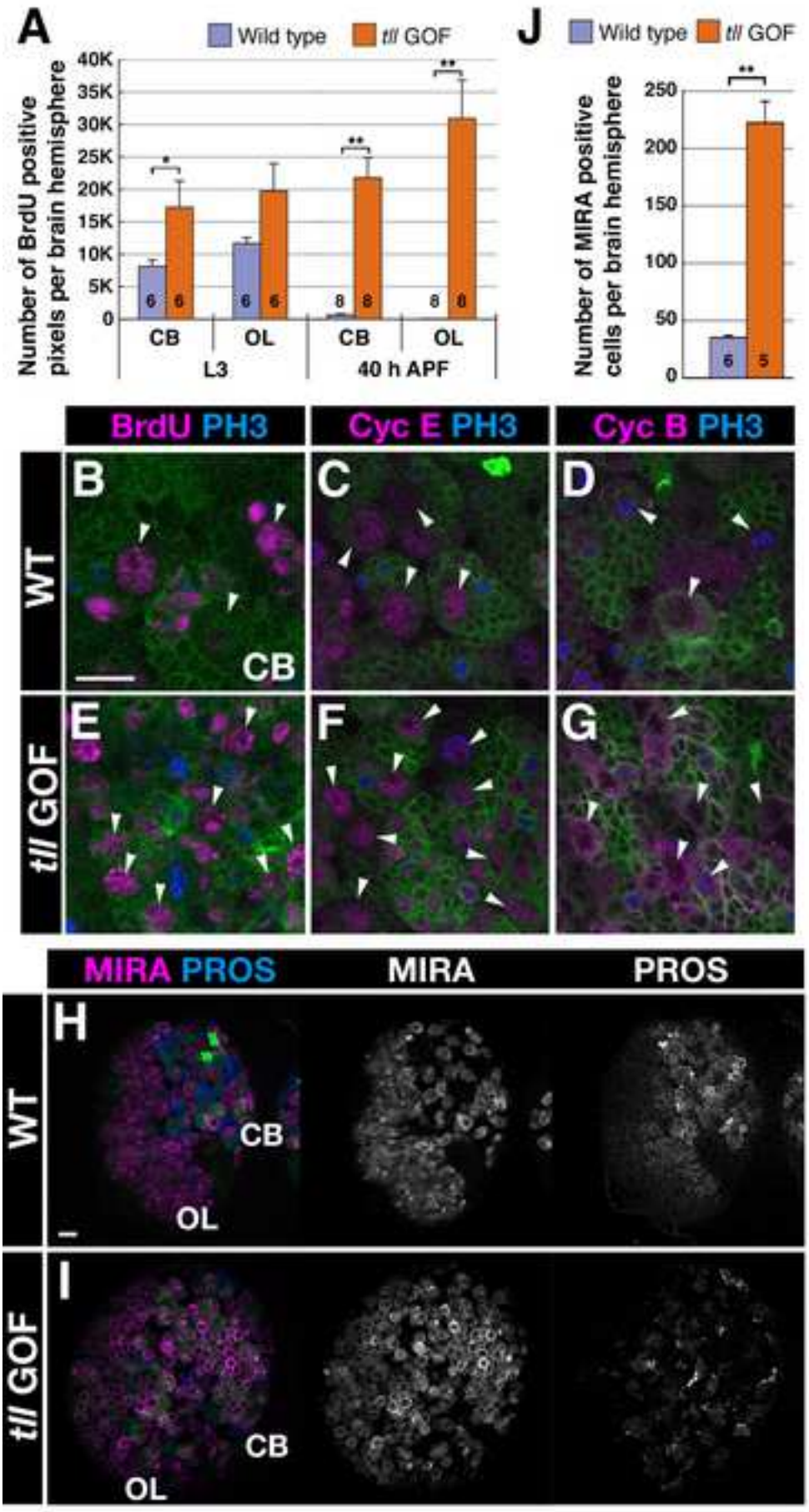

kurusu_Fig. 5

Figure 6

Click here to download high resolution image

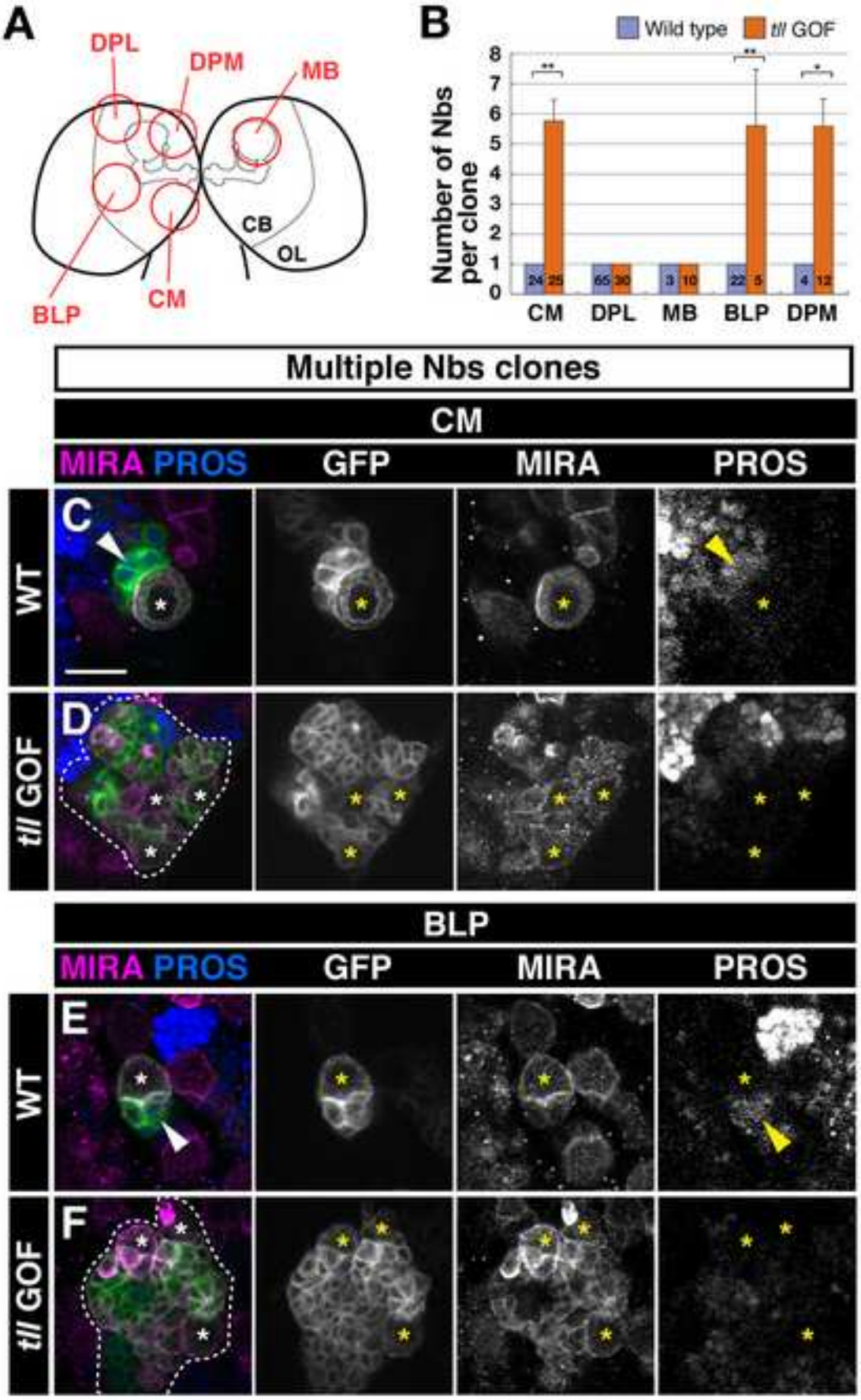

kurusu_Fig. 6

Figure 7

Click here to download high resolution image

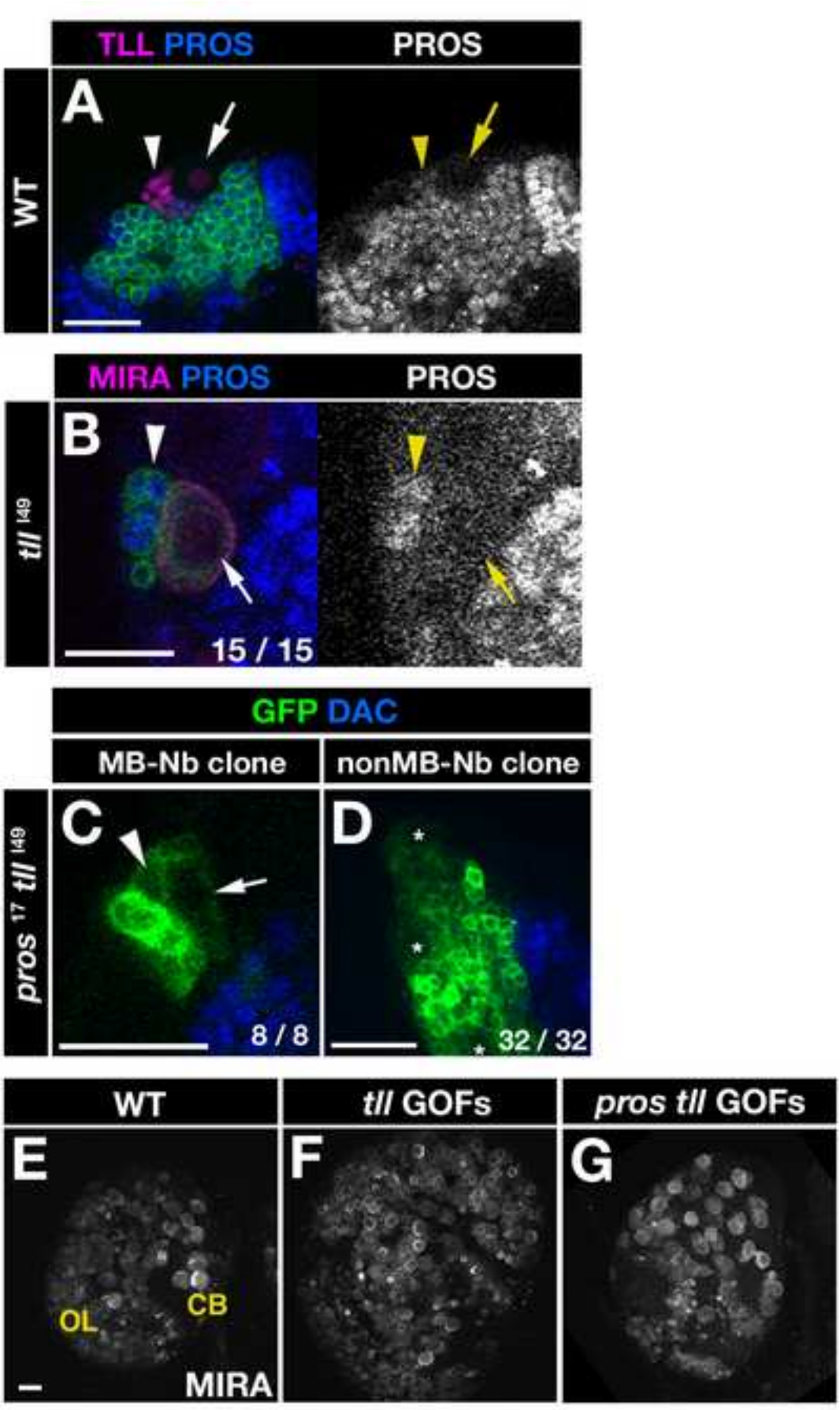

kurusu_Fig. 7